

3. Results

3.1. Grassland microenvironment in 1999

Figs. 6 to 9 display annual patterns of some microenvironmental factors observed in 1999 at a meteorological observation tower (MOT) at the grassland of the Environmental Research Center (ERC), University of Tsukuba, Japan.

The annual courses of the daily total and monthly mean solar radiation were not sinusoidal but fluctuated very sharply depending upon the degree of sky cloud cover (Fig. 6a). Concave in the curve indicates the *Baiu* rain period (from mid-June to mid-July) characterized by continuous cloudy and rainy days. Annual total solar radiation was 4807.2 MJ m^{-2} . Maximum daily solar radiation was 28.2 MJ m^{-2} (7 July). Midday (9:00 to 14:00 Japanese Standard Time, JST hereafter) mean value of albedo in the growing season was about 0.19. Minimum mean value of albedo (0.16) was observed during the senescence of the grassland. Albedo was affected by rain events to some extent (Fig. 6b).

Annual mean values of air temperatures and soil temperatures were $16.4 \text{ }^{\circ}\text{C}$ and $14.8 \text{ }^{\circ}\text{C}$, respectively. Fluctuations of air temperature (Fig. 7a) and soil temperature (Fig. 7b) followed a similar cosine pattern except that the shape of soil temperatures lagged behind about 20 days in peak values. Maximum and minimum of daily mean air temperature were $28.9 \text{ }^{\circ}\text{C}$ (27 Jul.) and $-0.9 \text{ }^{\circ}\text{C}$ (9 Jan.), respectively. Maximum and minimum of daily mean soil temperature were $28.2 \text{ }^{\circ}\text{C}$ (18 Aug.) and $3.5 \text{ }^{\circ}\text{C}$ (7 Feb.), respectively.

Annual mean wind speed was 0.9 m s^{-1} (Fig. 8a). Prevailing wind directions in growing season and in winter season were south to east and south to west, and north to east and north to west (Fig. 8b), respectively.

Annual total precipitation was 1194.2 mm, which is about 92% of mean precipitation in a normal year (Fig. 9a). Amount of precipitation in *Baiu* rain period was 327.5 mm (about 27% of total annual precipitation). Mean values of volumetric Soil water content (SWC) fluctuated from 0.32 to 0.70 across year with mean value of 0.45 (Fig. 9b). Appearances of peak values were associated with rain events. Maximum value of SWC (0.70, DOY 195) was observed in plum rain period. Due to rapid evapotranspiration from grasses and soil, SWC was depleted rapidly during growing season, especially after rain events. Bottom value periods of SWC were observed five times, DOY 125 to 168, DOY 195 to 216, DOY 217 to 225, DOY 226 to 264, and DOY 265 to 299, respectively. These periods roughly corresponded to the rapid growing period prior to plum rain period (DOY 125 to 168), the growing period after canopy closure (DOY 195 to 216, DOY 217 to 225, and DOY 226 to 264), the flowering period (DOY 265 to 299), respectively. Daily maximum, daily minimum, and annual mean values of the atmospheric evaporative demand were 1.45, 0.64, and 0.97, respectively (Fig. 9c). Monthly mean atmospheric water vapor pressure deficit (*VPD*) was largest in August when there was little rain and plants consumed much water. No violent water stress was observed during the growing season of the grassland.

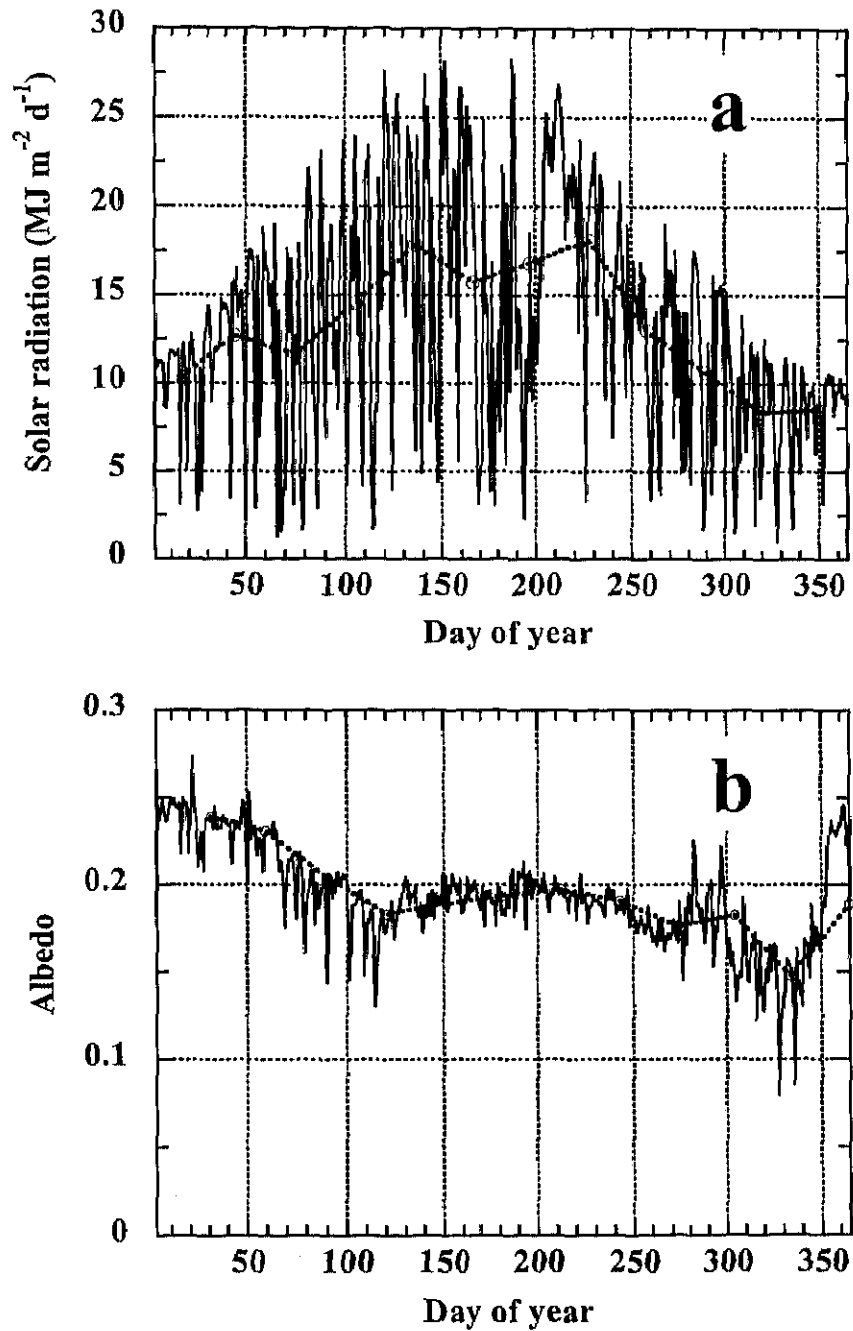


Figure 6. a: Daily total recipient solar radiation and monthly mean recipient solar radiation (dashed line with empty circles). b: Midday (9:00 to 14:00 Japanese Standard Time, JST) average short wave reflection (albedo) of the grassland. Lines with empty circles indicate monthly mean values. Albedo data are from Higuchi et al., 1999, 2000.

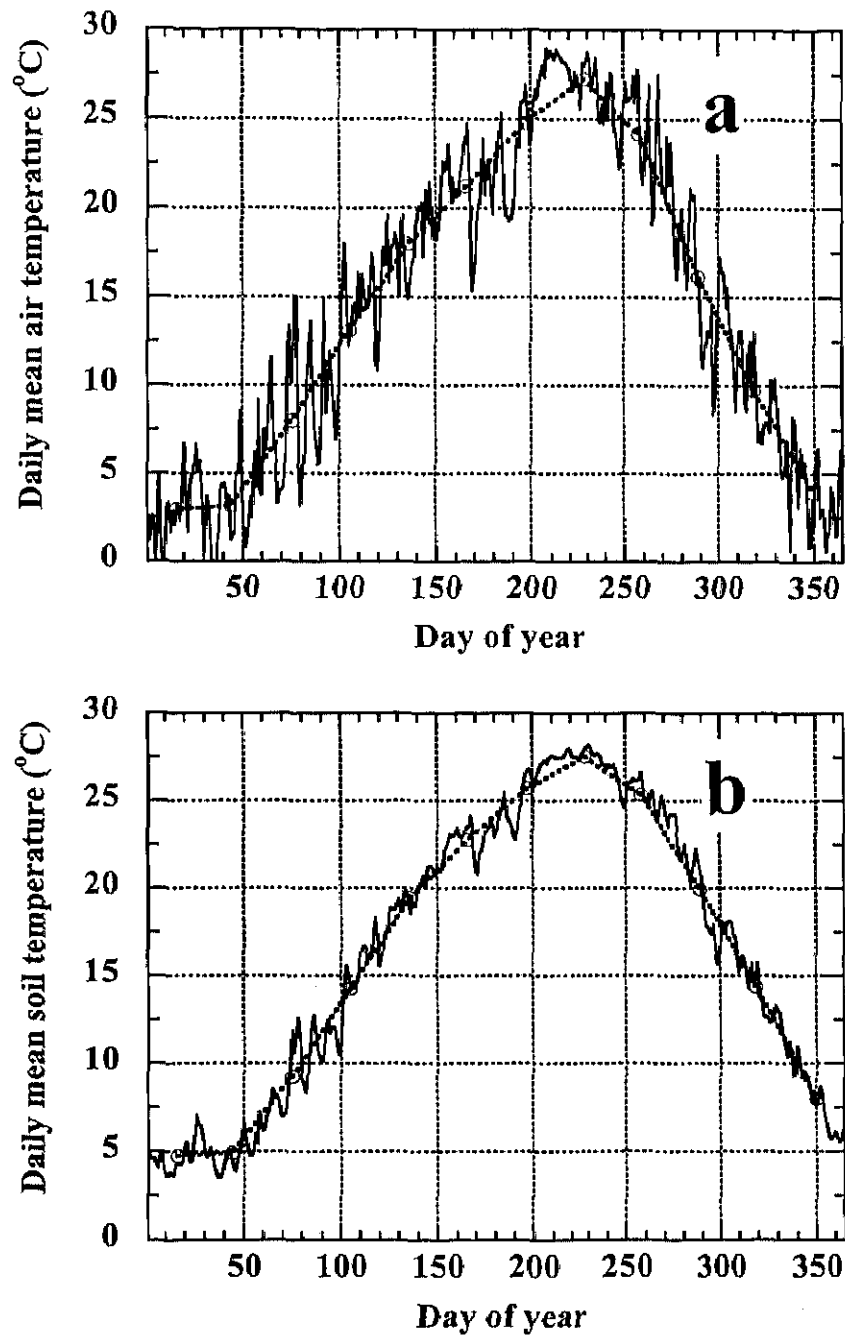


Figure 7. a: Daily mean air temperatures at a height of 1.6 m above the ground. b: Daily mean soil temperatures at a depth of 0.02 m beneath the ground. Lines with empty circles indicate monthly mean values.

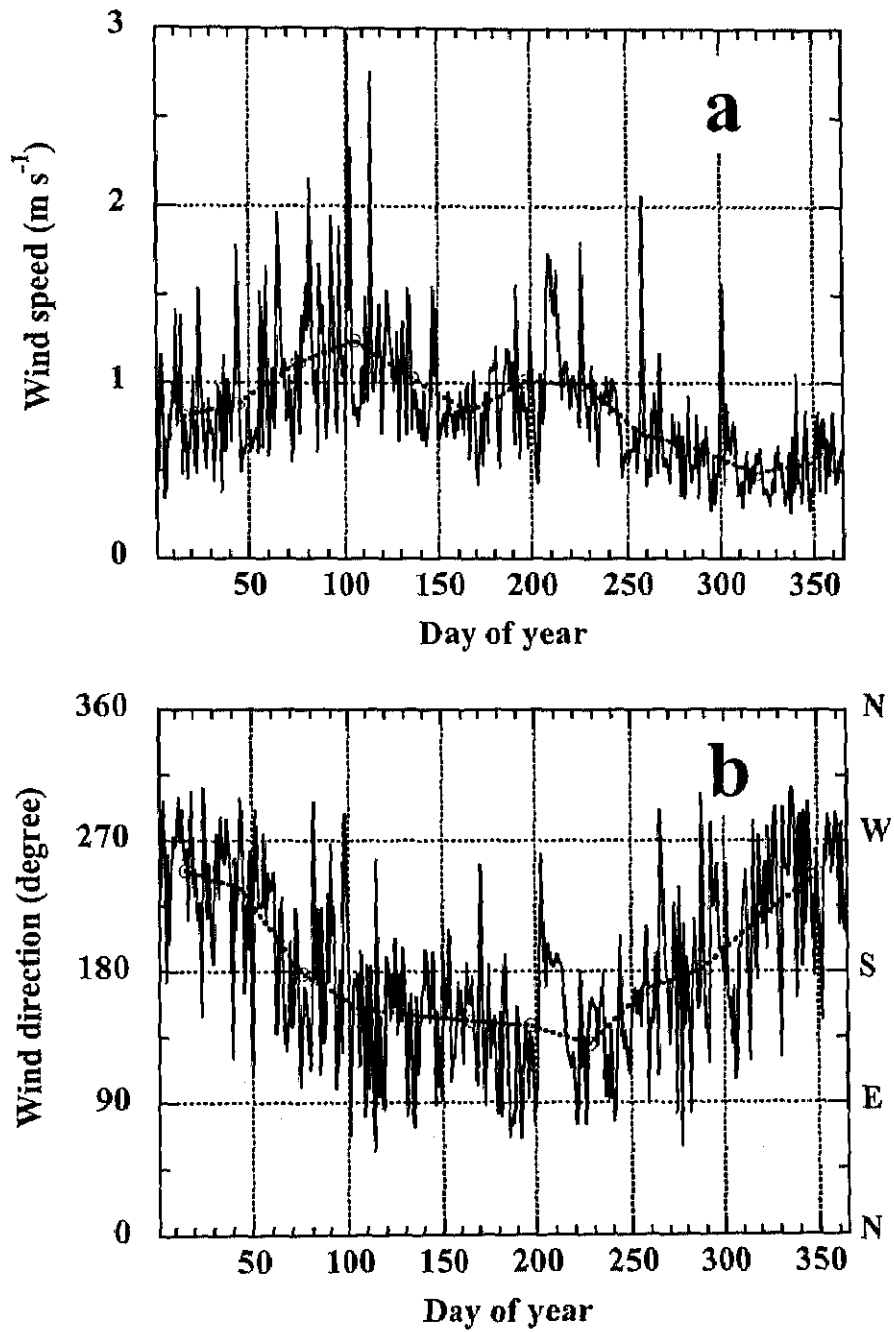


Figure 8. a: Daily mean wind speeds at a height of 1.6 m above the ground. b: Daily mean wind directions. Lines with empty circles indicate monthly mean values.

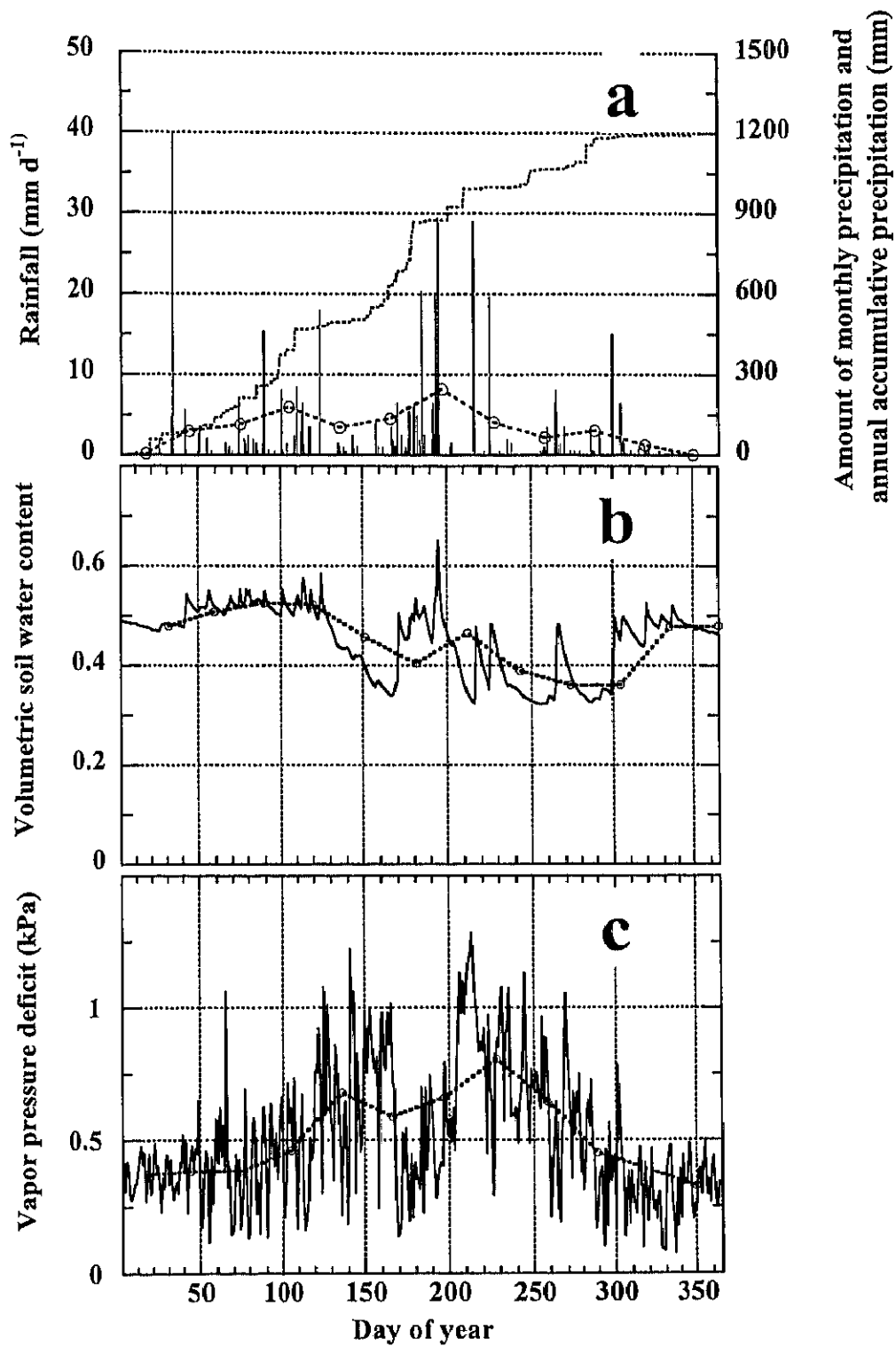


Figure 9. a: Precipitation (vertical lines, dashed line with empty circles, and dashed line without marks indicate amounts of daily integrated, monthly integrated, and annual accumulative precipitation, respectively). b: Daily mean volumetric soil water content (SWC) in the upper 15 cm of soil. c: atmospheric vapor pressure deficit (VPD) at 1.6 m.

3.2 Canopy height and leaf area index in 1999

Grasses sprouted in the late March and grew very rapidly until late July when h_c reached its peak value, exceeding 1.0 m (Fig. 10a). The height growth rate was largest during DOY 160 to 180 (roughly corresponding to the *Baiu* rain period). Plumes in curves of h_c and the height growth rate after DOY 250 (Fig. 10a) were due to flowering growth of *Miscanthus sinensis* (C4) and *Solidago altissima* (C3). h_c was decreased due to lodging of *Festuca arundinacea* (C3) in late September and early October.

LAI increased gradually from May to early August when it reached its maximum of around 5.53 (Fig. 10b). From then through early October LAI remained constant around 5.50, and began to decrease from mid October because of senescence but the canopy analyzer (LI-2000) failed to monitor this change accurately. Seasonal variation of the leaf area expansion rates followed a similar pattern as the height growth rate, with peak values being observed during DOY 160 to 180, which was the same period that the peak values of the height growth rate occurred. The canopy closed when LAI reached around 3 (late June).

A high correlation existed between LAI and h_c (Fig. 11). LAI can be calculated from a linear regression on h_c (m):

$$LAI = 7.24 h_c - 1.35 \quad (n = 13, r^2 = 0.99, h_c > 0.2 \text{ m}) \quad (23)$$

Based on analysis of h_c , LAI and field observation of phenology of some dominant species of the grassland, in the following discussion, the growing season will be roughly (arbitrarily sometimes) classified into 5 periods: Rapid growth period or period prior to canopy closure (DOY 101 to 166), *Baiu* rain period with canopy closure (DOY 167 to 195), closed canopy period after the *Baiu* rain and before flowering (DOY 196 to 270), flowering period of most plants (DOY 271 to 290), and senescence period (DOY 291 to 346).

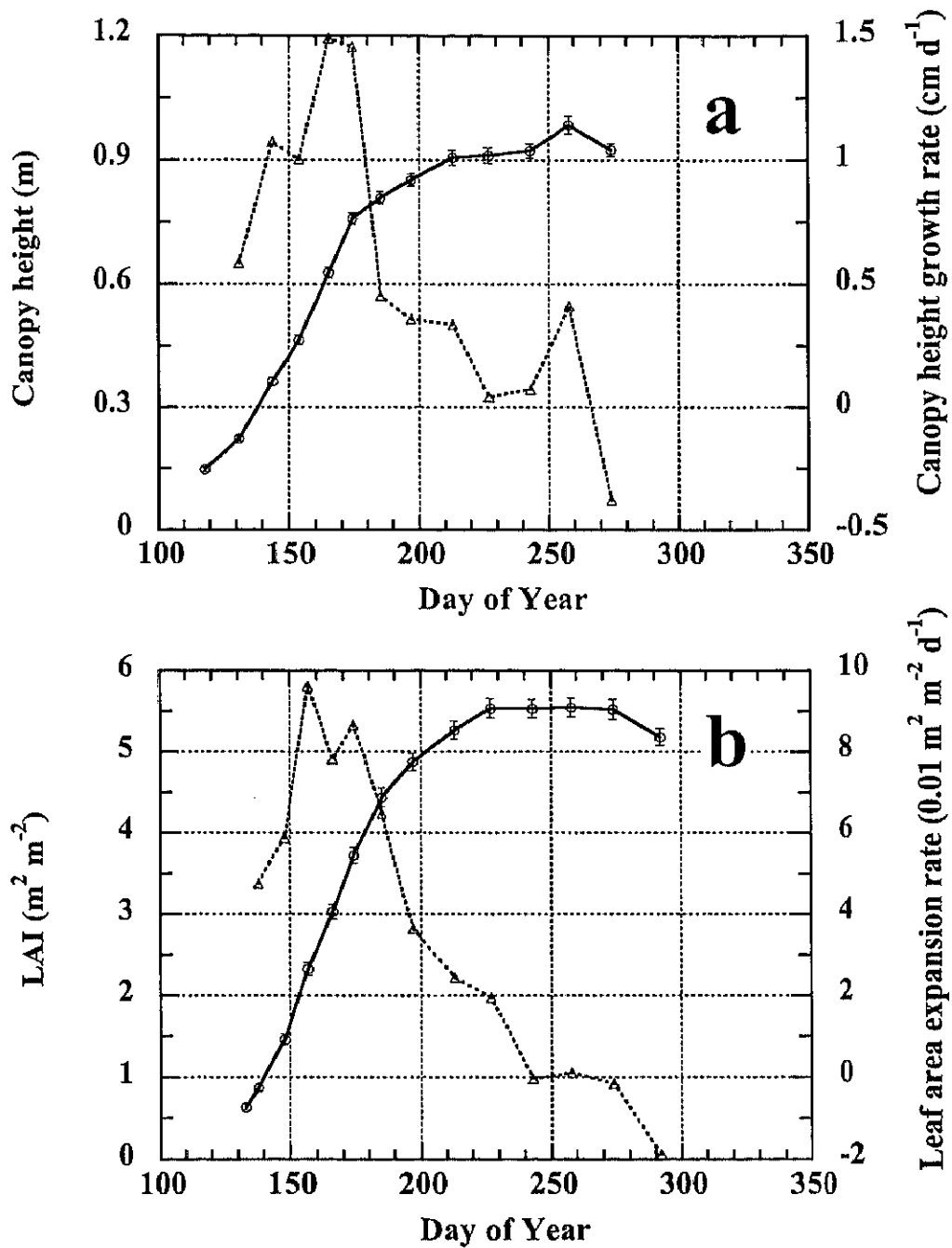


Figure 10. a: Seasonal patterns of canopy height (h_c in m, solid line) and height growth rate (in cm d^{-1} , dashed line with empty triangle) of the ERC grassland in 1999. b: Seasonal variations in leaf area index (LAI, solid line) and leaf area expansion rate (in $0.01 \text{m}^2 \text{m}^{-2} \text{d}^{-1}$, dashed line with empty triangle). Vertical bars indicate standard errors.

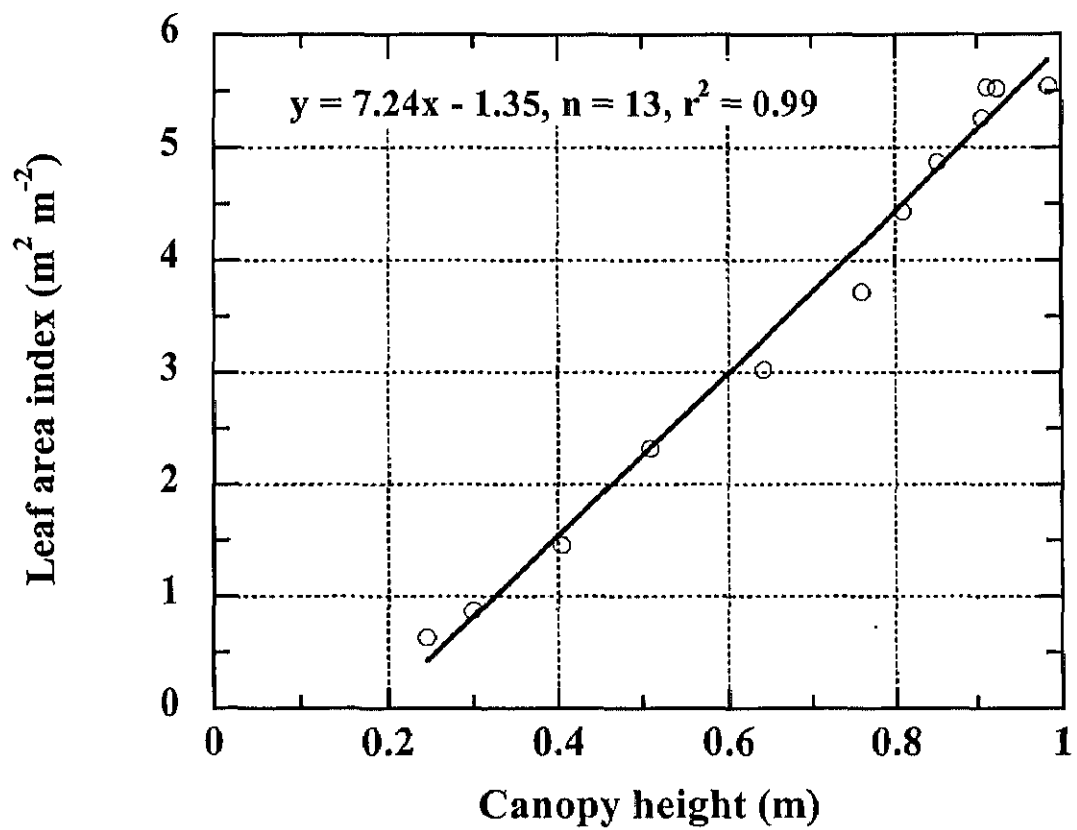


Figure 11. The relationship between leaf area index (LAI) and canopy height (h_c). The line in the figure is a line of best fit with $LAI = 7.24 h_c - 1.35$ ($n = 13, r^2 = 0.99, h_c > 0.2$ m)

3.3 Performance of the eddy flux measurement system

Our EC measurement system well monitored fluctuations in vertical wind speed (w), air temperature (T), specific humidity (q) and CO₂ concentration (c) over the ERC grassland (Fig. 12). The four scalars (w , T , q and c) fluctuated in a similar manner with a high degree of correlation and followed closely in phase. CO₂ and the specific humidity displayed similar fluctuations but in opposite phase. The recorded signals show that w , T , q and c fluctuated about 2 m s⁻¹, 5 °C, 3 g kg⁻¹, and 10 ppm, respectively (Fig. 12). The magnitude of the scalar fluctuations depended on the direction of the vertical wind speed. These observations are consistent with those made by Ohtaki (1984) and Verma et al. (1992b).

In addition, we employed two methods to assess the performance of our EC measurement system: Energy balance closure check and comparison to lysimeter.

Closure of the energy budget was employed to assess the overall performance of our eddy flux measurement system. This was done on two time scales, i.e. daily integrals and hourly means. Prior to the senescence of grasses, the sum of the latent heat and sensible heat flux densities measured with the eddy correlation technique ($H + LE$) matched satisfactorily the available energy ($Q_n = R_n - G$) both on the hourly averaged basis and on the daily averaged basis (Fig. 13a). Hourly energy budget closure check indicates $H + LE = 1.01 Q_n \text{ W m}^{-2}$ ($r^2 = 0.90$) for 2251 hourly periods. The regression slope was almost unity, implying almost complete closure of the energy balance. Daily energy budget closure check indicates $H + LE = 1.04 Q_n \text{ MJ m}^{-2} \text{ d}^{-1}$ ($r^2 = 0.81$) for 86 days (Fig. 13b). The regression slope in the literature is generally within the range of 0.8 to 1.1 (e.g. Baldocchi, 1994a; Baldocchi and Harley, 1995; Blanken et al., 1997; Jarvis et al., 1997; Kelliher et al., 1998; Lafleur, 1999; Lee and Black, 1993; Verma et al., 1992b). Our flux measurement system had thus relatively small system noise and would be reliable in estimating eddy fluxes in the grassland.

Although the closure was perfect from the viewpoint of long-term measurements, it varied when data sets were grouped on a daily basis according to the growth stages of the canopy (Fig. 14). There was about 4% underestimation in $H + LE$ during the rapid growth period (A in Fig. 14). During the closed canopy period and the flowering period $H + LE$ was overestimated by 6% and 10%, respectively (B and C in Fig. 14). About 42% of underestimation of $H + LE$ was observed during the senescence period (D in Fig. 14).

Reliability of the latent heat flux densities estimated by the EC technique was also checked against those measured by the micro-lysimeter. Prior to the senescence of grasses, the latent heat flux densities estimated by the EC technique agreed well with those directly measured with the lysimeter (Fig. 15). The large influence of wind on instantaneous measurements contributed to the scatter in the figure. Linear regression indicates that $LE (EC) = 1.00 LE (Lysimeter)$ ($r^2 = 0.85$) for 2193 hourly periods (Fig. 15). This relationship was also subject to seasonal variation of the grassland canopy (data not shown). Good agreement between the EC-measured LE and lysimeter-measured LE can be also reflected in their daily courses (Fig. 16). The EC technique estimated exactly the latent heat flux densities from the closed canopy to the beginning of senescence, but could not estimate LE correctly during the senescence period of grasses.

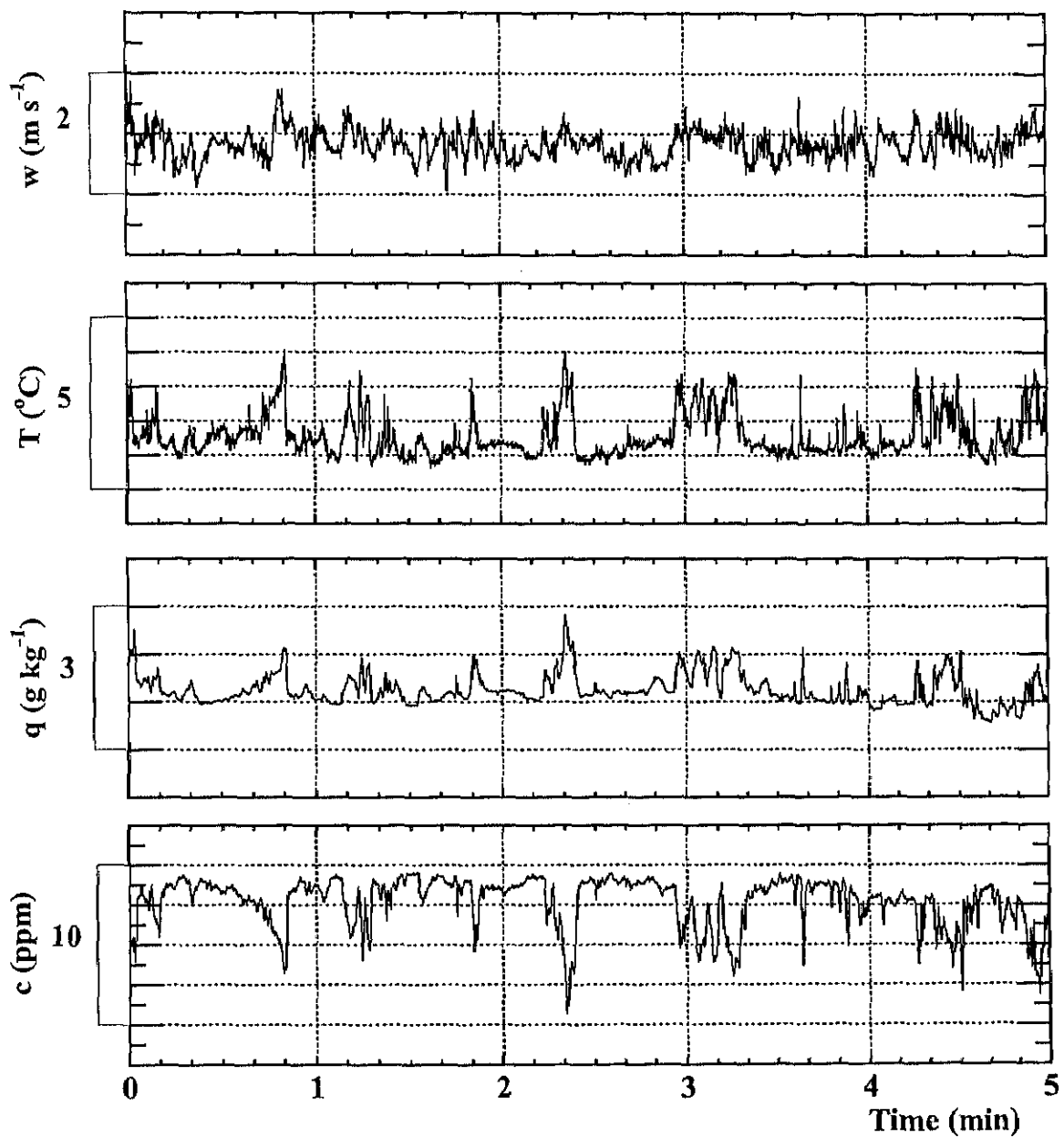


Figure 12. Typical time traces of turbulent fluctuations in vertical wind speed (w), air temperature (T), specific humidity (q), and carbon dioxide concentration (c) over the ERC grassland from 1102 to 1107 (5 min) on 8 June, 1999.

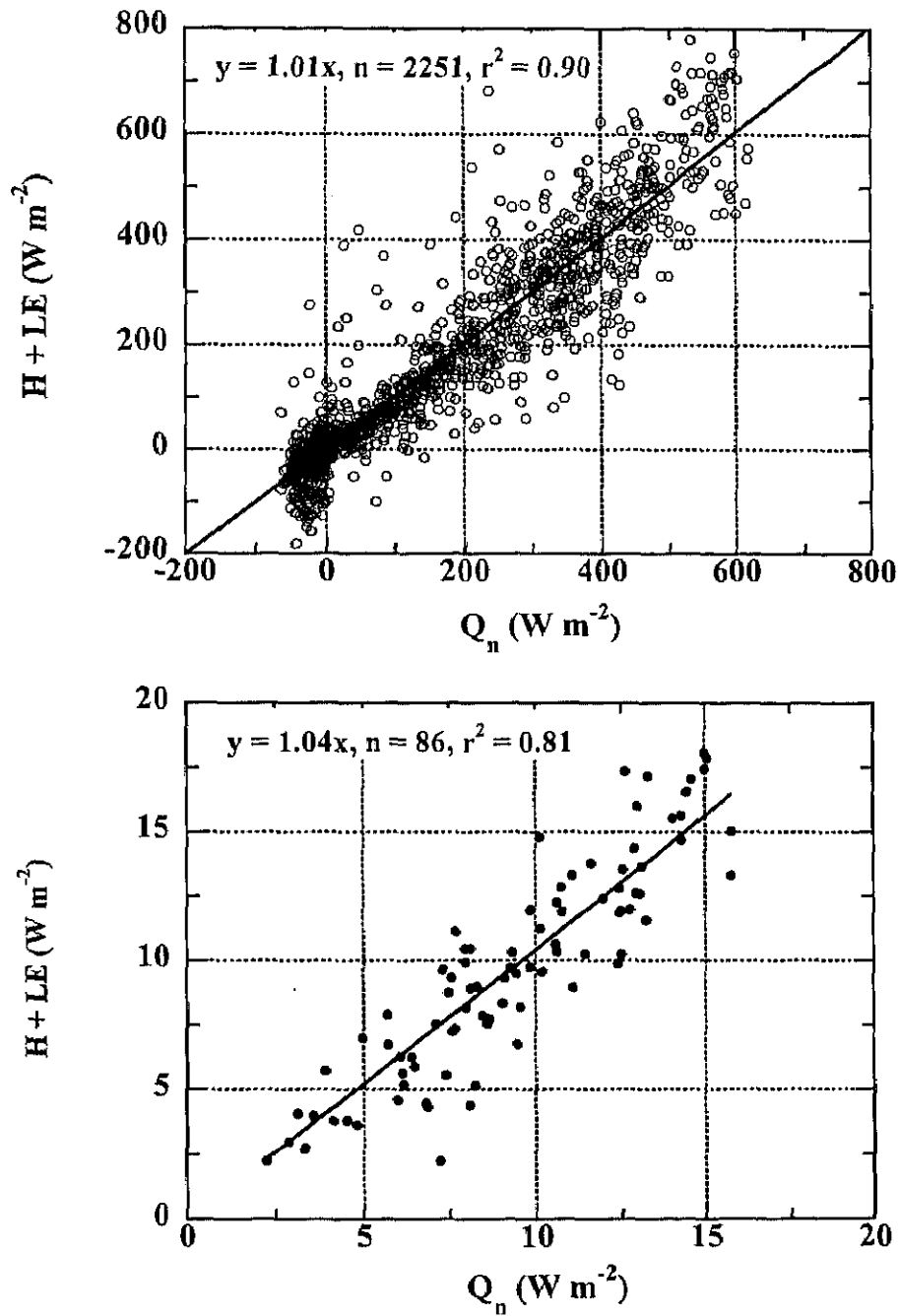


Figure 13. a: Hourly energy budget closure check. b: Daily energy budget closure check. $R_n - G$ is the net available energy flux density (Q_n) to the canopy, measured directly. The sensible heat (H) and latent heat (LE) flux densities were measured with the eddy correlation technique. Only data prior to the senescence period were included. The relationship between Q_n and $H + LE$ is expressed by the linear regression equation: $H + LE = 1.01Q_n$, $n = 2251\text{h}$, $r^2 = 0.90$ on the hourly basis; $H + LE = 1.04Q_n$, $n = 86$, $r^2 = 0.81$ on the daily basis.

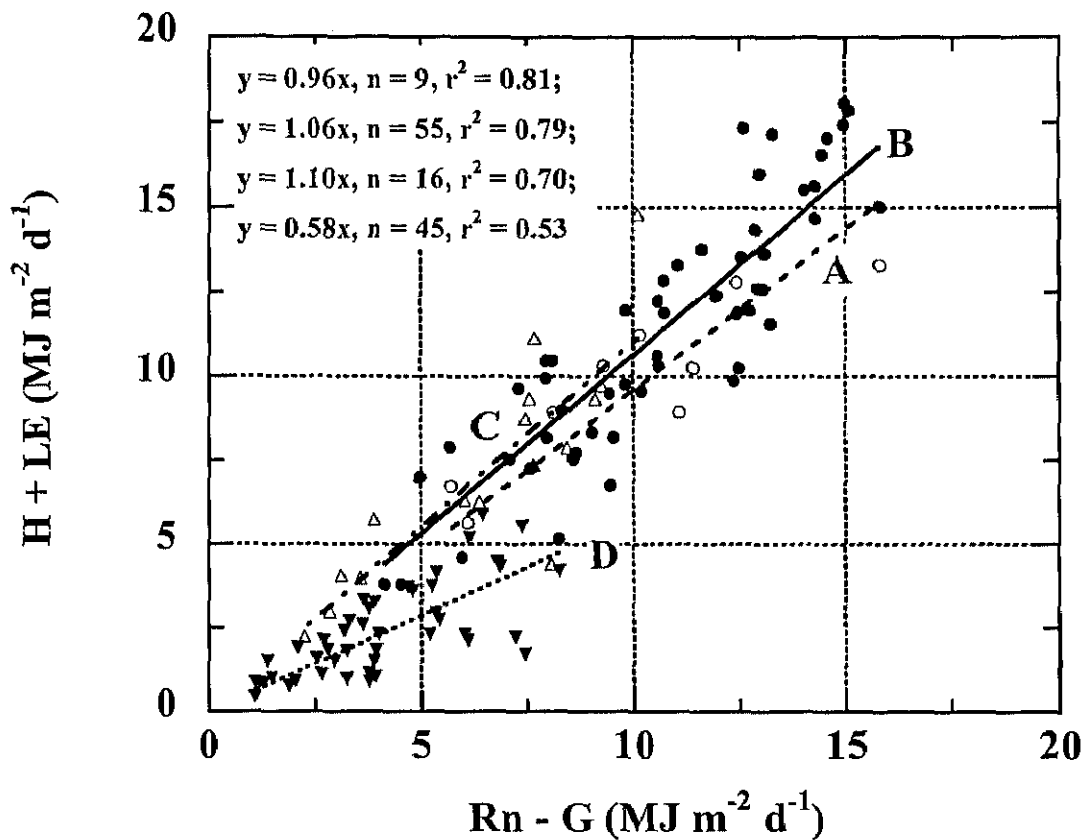


Figure 14. Daily performance of the eddy flux measurement system, as indicated by the closure check, varied in different growing periods of the canopy. $R_n - G$ is the net available energy to the canopy, measured directly. The sensible heat (H) and latent heat (LE) flux densities were measured with eddy correlation technique. The relationship between Q_n and $H + LE$ is expressed in linear regression equations as: $H + LE = 0.96Q_n$, $n = 9$, $r^2 = 0.81$ for the period prior to closed canopy (\circ); $H + LE = 1.06Q_n$, $n = 55$, $r^2 = 0.79$ for the closed canopy period after the *Baiu* rainy season and before flowering (\bullet); $H + LE = 1.10Q_n$, $n = 16$, $r^2 = 0.70$ for the flowering period (\triangle); and $H + LE = 0.58Q_n$, $n = 45$, $r^2 = 0.53$, for the senescence period (\blacktriangledown), respectively.

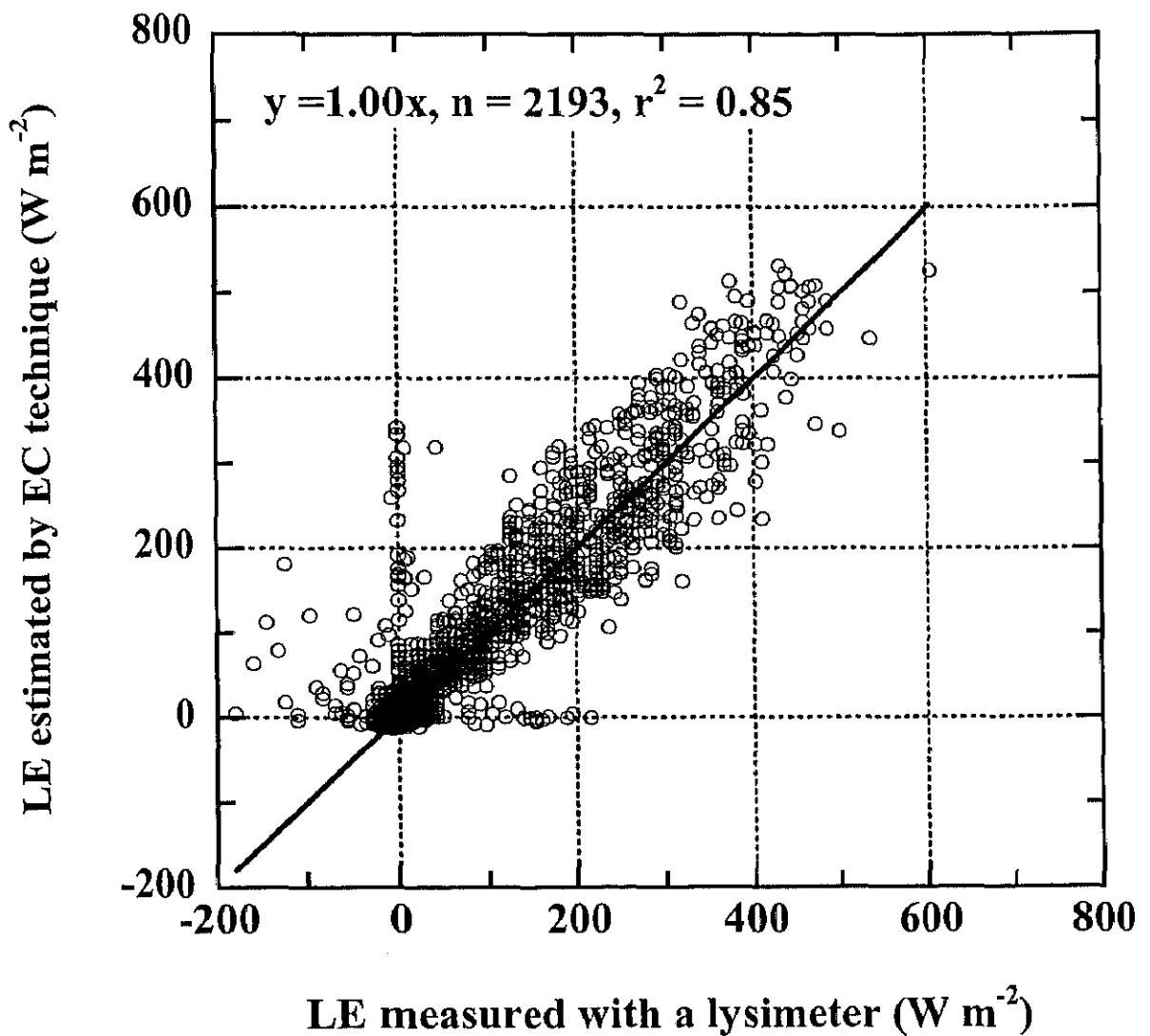


Figure 15. Comparison between the latent heat flux densities estimated by the EC technique and those measured directly by a lysimeter on an hourly basis during the measurement period prior to the senescence of grasses in 1999. LE from the entire measurement period except for rainy days are plotted against LE measured by lysimeter. The relationship is expressed as a linear regression equation: LE (EC) = 1.00 LE (lysimeter), $n = 2193$ h, $r^2 = 0.85$.

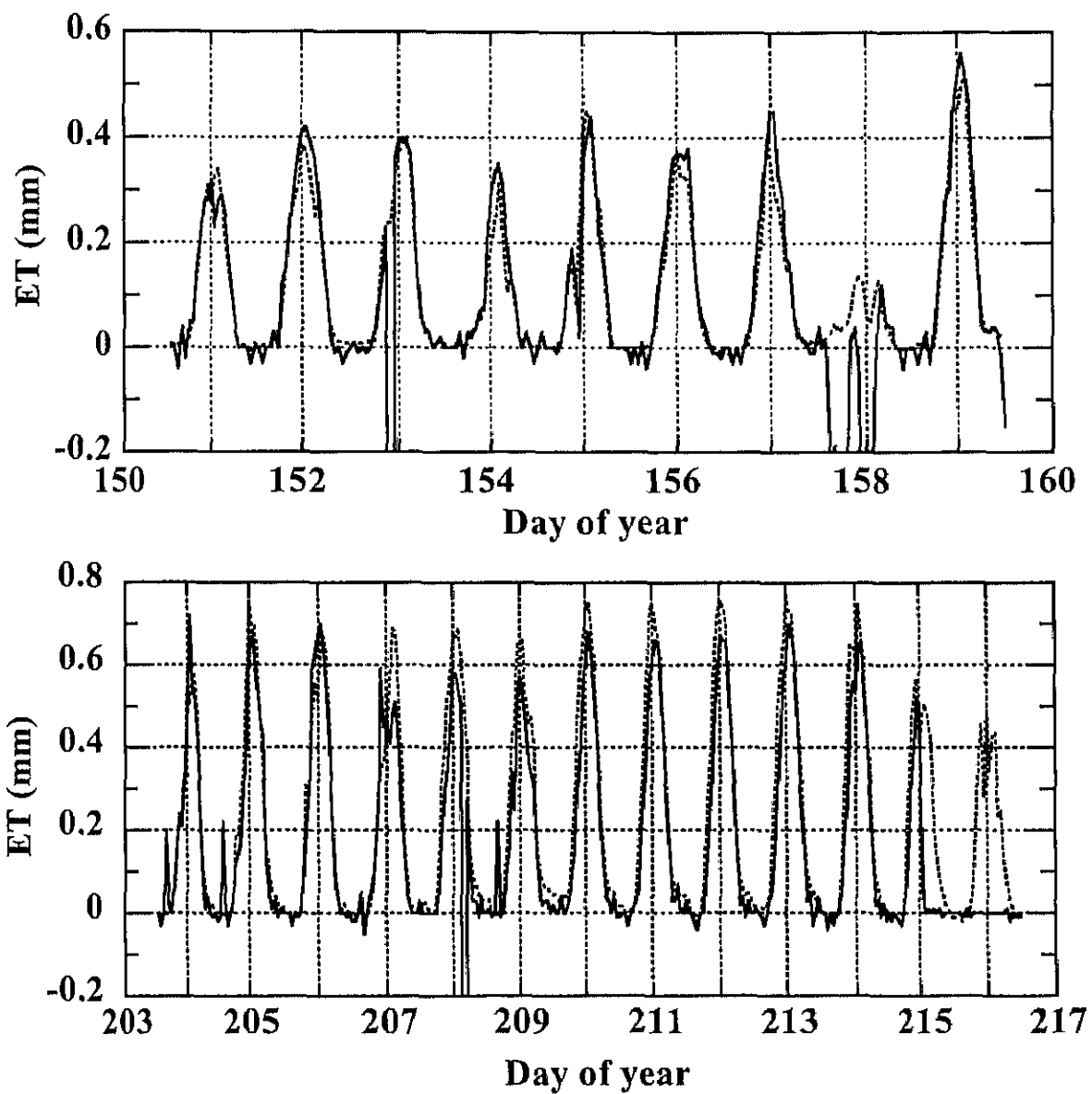


Figure 16. A comparison of the diurnal sequences between evapotranspiration rate (ET) estimated by the EC technique (broken line) and that measured directly by a lysimeter (solid line). a: DOY 151 to 159 in the rapid growth period; b: DOY 204 to 216 in the early part of the closed canopy period.

3.4 Diurnal patterns of the partitioning of available energy

We expected that the development of the grassland canopy exerted a pronounced influence on how the available energy (Q_n) and its partitioning into latent heat (LE) and sensible heat (H) flux densities. The diurnal variations in Q_n , LE and H measured over the grassland canopy present large differences in magnitude at different growth stages (Figs. 17 to 21). Daily courses in Q_n generally followed a sinusoidal pattern, similar to the pattern for solar radiation (R_s), implying a close relation of Q_n to R_s although the magnitude of Q_n was associated with the canopy properties. Q_n reached its maximum around 11:00 JST, corresponding roughly to solar noon. Diurnal trends in LE approximately followed those in Q_n , but peak values of LE tended to appear 1 to 2 h later than Q_n did, resulting in an asymmetrical distribution of LE . This hysteresis seemed to correspond to micrometeorological events that occurred during the afternoon hours, for example, higher air temperatures, larger atmospheric evaporative demand (vapor pressure deficit, VPD), and stronger winds (effective turbulent mixing). LE behaved in a similar fashion as VPD (Figs. 17 to 21). Winds generally reached their peak velocities in mid afternoon hours (Figs. 17 to 21). Daily pattern of H was different from Q_n and LE in that H generally peaked before solar noon and switched sign approximately 1 to 2 h earlier than LE or Q_n in the late afternoon hours. Higher values of H during the morning hours were related to lower wind speeds and lower VPD. On the other hand, lower or negative values of H during the late afternoon hours were very possibly associated with concurrence of higher air temperatures, stronger winds, and larger VPD, resulting in mild sensible heat advection (SHA) (Anderson et al., 1986; Rosenberg et al., 1983). SHA may have somewhat contributed to the asymmetrical distribution of LE in the afternoon compared to the morning hours. SHA (directed towards the canopy surface) generally enhances evapotranspiration as a result of additional energy to the energy budget (Rosenberg et al., 1983). Similar results are also reported in Baldocchi et al.

(1981c) for soybean, and in Anderson and Verma (1986) for sorghum. This phenomenon was not significant on cloudy days.

Nighttime values of Q_n , LE and H were quite small (generally less than 50 W m^{-2}) throughout the growing season of the grassland canopy as compared to their daytime values. One very possible reason was that they were inherently underestimated by the EC technique under stable conditions (inverse gradient) (e.g. Dyer et al., 1982).

Dark evapotranspiration was generally positive (directed away from the canopy surface) at most times of night except for the very early morning hours during most of measurement period; this may be due to contribution of negative sensible heat flux and soil heat flux to evapotranspiration of water from the surface. The patterns for LE we observed were similar to those reported for a boreal wetland (Lafleur et al., 1997) and for a lake (den Hartog et al., 1994).

The available energy partitioned into its components rather differently at different growth stages of the canopy. During the period prior to canopy closure of the ERC grassland (DOY 151-159), hourly peak values of the available energy (Q_n) ranged from 350 to 500 W m^{-2} (Fig. 17a). Large part of Q_n was partitioned into the evaporative fraction (EF , expressed as LE/Q_n). Midday values (09:00 to 14:00 JST, the same hereafter) of EF were more than 50%. Midday Bowen ratio (β , expressed as H/LE) in this period was generally larger than 0.50. Peak values of atmospheric VPD ranged between 1.5 and 2.5 kPa (Fig. 17b).

During the early part of the closed canopy period (DOY 204 to 216), hourly peak values of Q_n were generally between 500 and 600 W m^{-2} (Fig. 18a). LE was strongly coupled with Q_n during this period. The percentage of Q_n consumed by LE was fairly high. Midday values of EF were generally larger than 80%. The highest midday EF value of nearly 90% was observed in this period (DOY 209), which is reasonable because the ERC grassland was not water-limited (the volumetric soil water content was generally larger than 0.35). The sensible heat flux density was a very minor part in Q_n ; the maximal midday mean value of H proportion was about 34%. Midday Bowen ratio

in this period was lower than 0.35. Peak values of VPD varied between 1.8 and 2.5 kPa (Fig. 18b).

During the later part of the closed canopy period (DOY 241 to 255), hourly peak values of Q_n varied between 300 and 550 $W m^{-2}$ depending upon incoming solar radiation (Fig. 19a). EF still dominated Q_n during this period. Midday values of EF were generally larger than 60%. Midday Bowen ratio in this period was lower than 0.50. Peak values of VPD varied between 1.3 and 2.0 kPa (Fig. 19b).

During the flowering period (DOY 271 to 290), hourly peak values of Q_n varied between 200 and 450 $W m^{-2}$ (Fig. 20a). About half of Q_n was partitioned into LE and the other half into H . During this period H became the main consumer of Q_n . Midday values of EF were generally less than 50%. Midday Bowen ratio in this period increased to larger than unity, suggesting that the energy partitioning was H -dominated. Peak values of VPD varied between 1.0 and 2.0 kPa (Fig. 20b).

As the grasses entered the senescence period (DOY 291 to 304), hourly peak values of Q_n varied between 100 and 320 $W m^{-2}$ (Fig. 21a). Midday values of EF were generally less than 30%. A larger proportion (about two thirds) of Q_n was partitioned into H . Midday Bowen ratio in this period was larger than 1.5. Reduction of the EF during the senescent period could be explained partly in terms of diminishment of effective evaporative leaf area, which could not be discerned by the LI-2000 canopy analyzer. Peak values of VPD varied between 0.5 and 1.6 kPa (Fig. 21b).

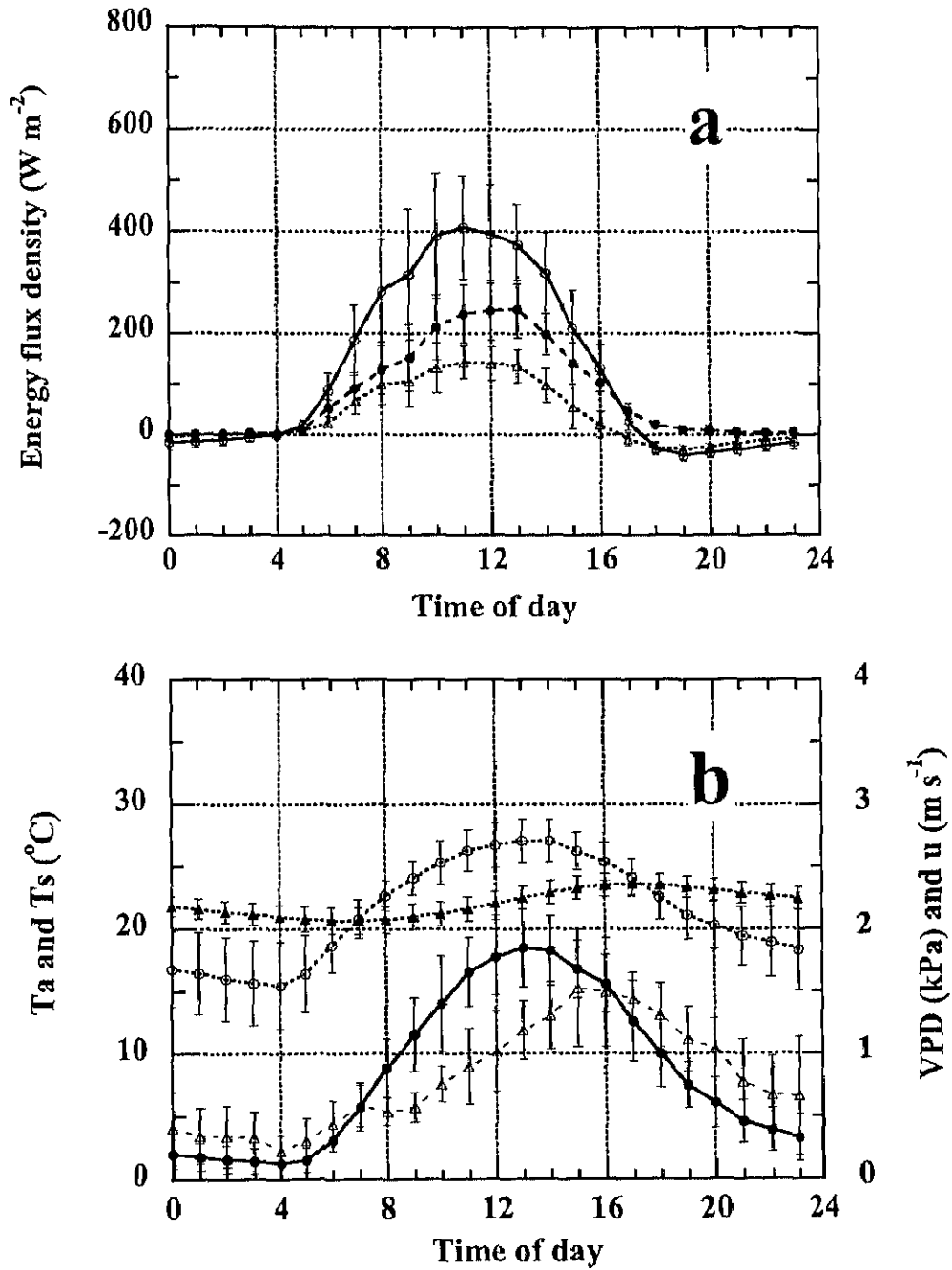


Figure 17. Daily variations in energy flux densities and some microenvironmental variables. a: Daily sequences of available energy (Q_n , solid line with \circ) and its partitioning into latent heat (LE , heavy dashed line with \bullet) and sensible heat (H , light dashed line with \triangle) flux densities. b: Daily variations in air temperature at 1.6 m (T_a , \circ), soil temperature at depth of 2 cm (T_s , \blacktriangle), vapor pressure deficit (VPD, \bullet), and wind speed at 1.6 m (u , \triangle). Data are hourly averages over selected 9 days (DOY 151 to 159) during the period prior to canopy closure ($\text{LAI} = 2.13$, $\text{SWC} = 0.38$).

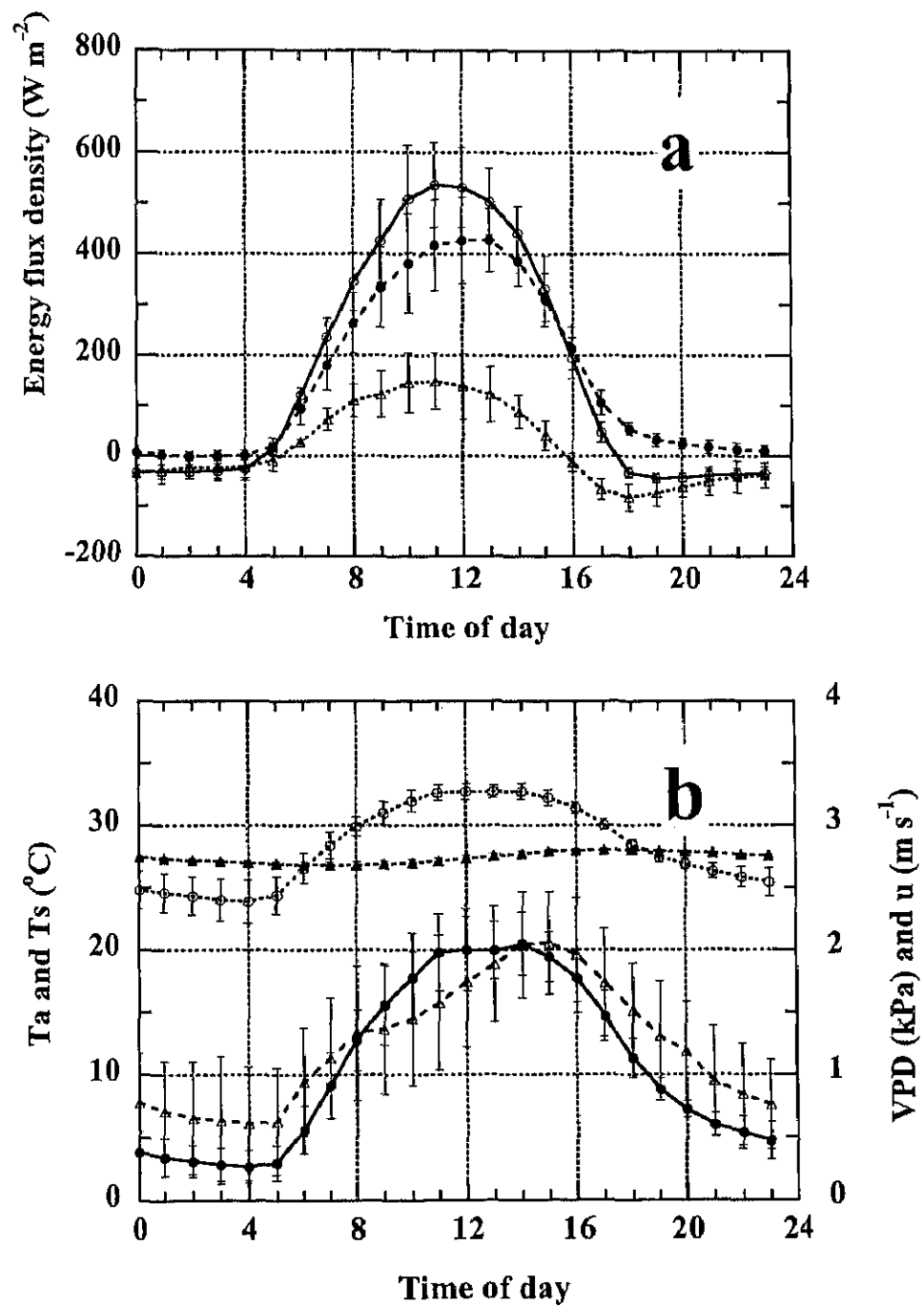


Figure 18. Same as Fig. 17 but for the selected 13 days (DOY 204 to 216) in the early part of the closed canopy period ($LAI = 5.25$, $SWC = 0.37$).

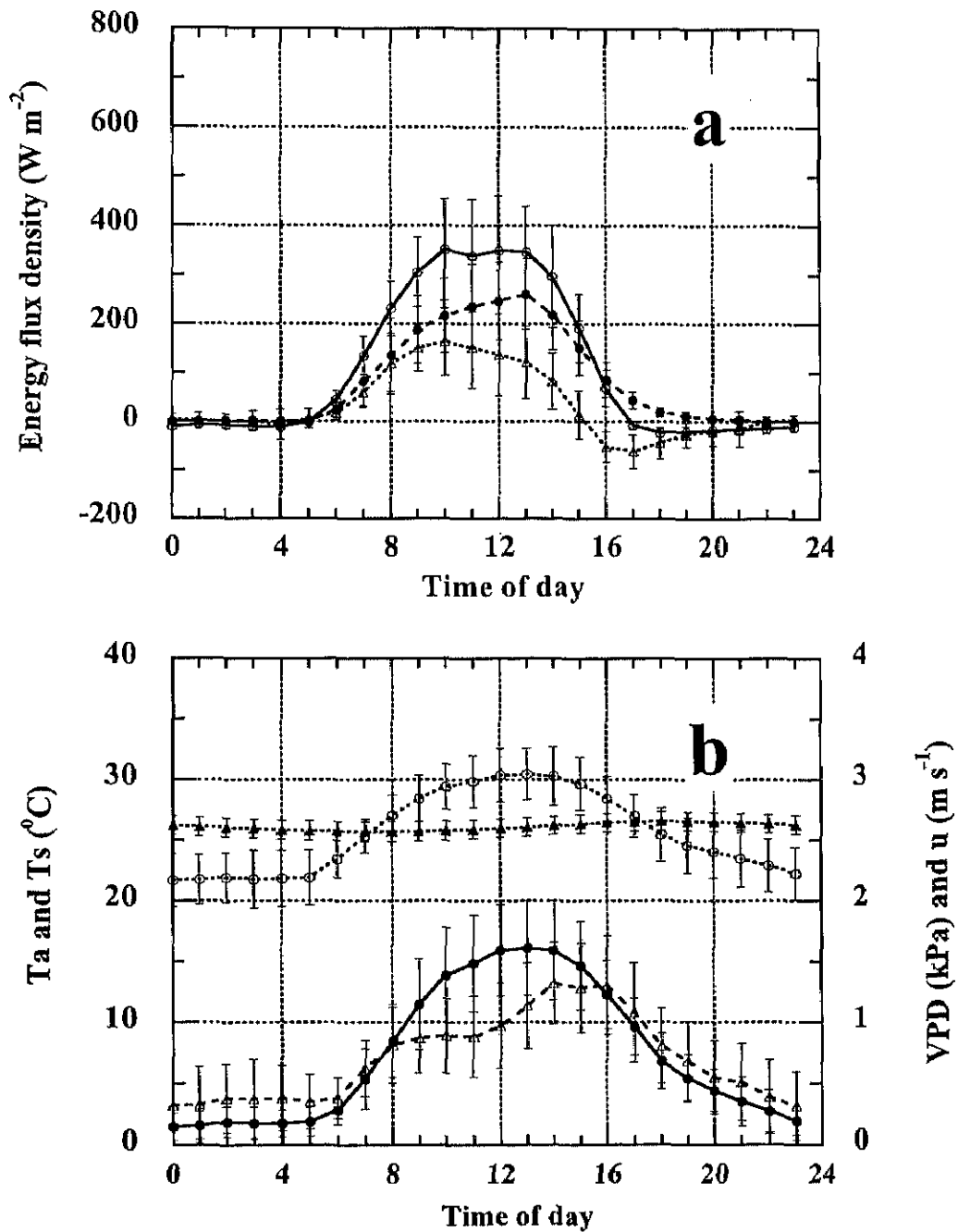


Figure 19. Same as Fig. 17 except for 15 selected days (DOY 241 to 255) in the later part of the closed canopy period ($LAI = 5.50$, $SWC = 0.33$).

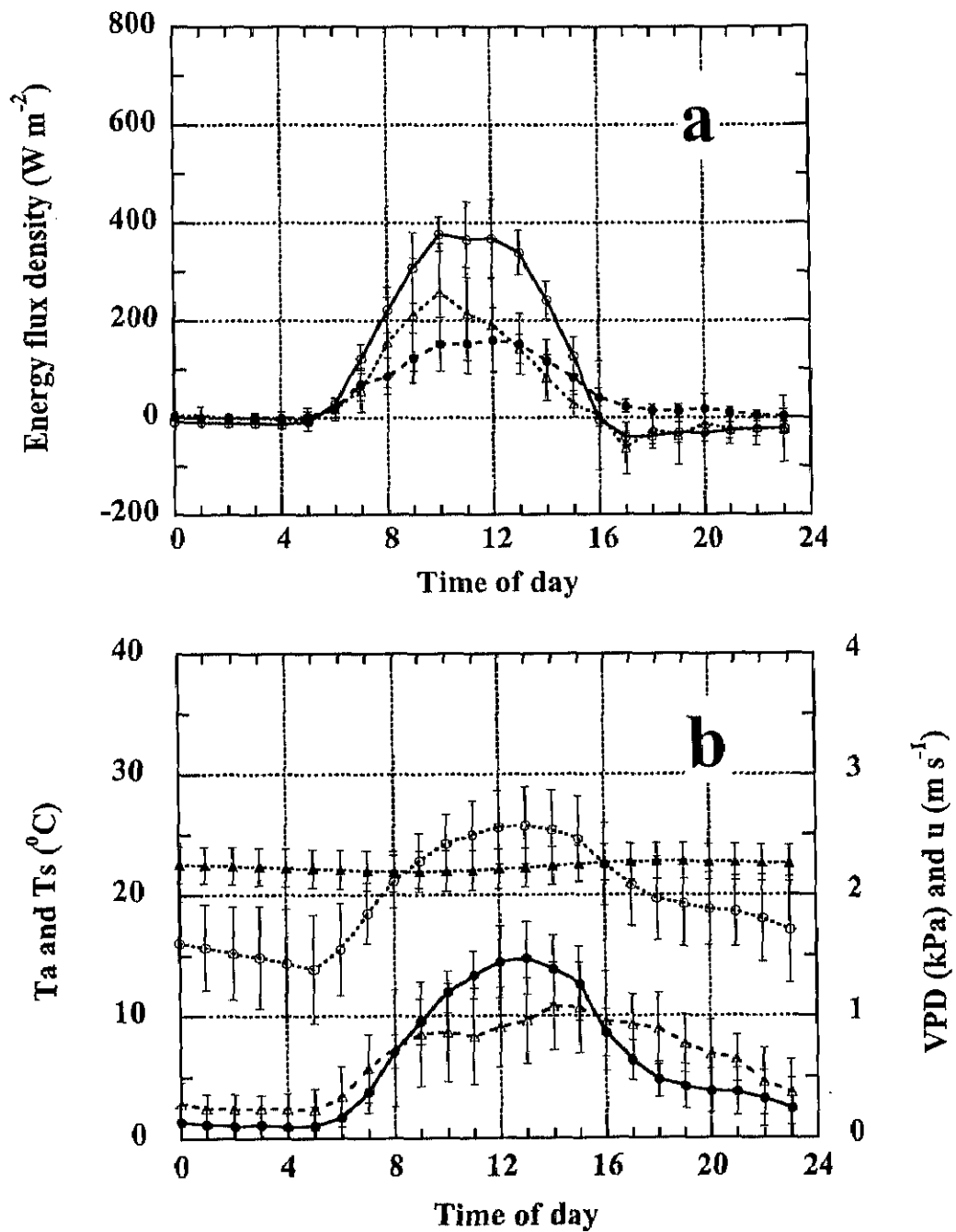


Figure 20. Same as Fig. 17 but for 8 selected days (DOY 271 to 290) in the flowering period (LAI = 5.37, SWC = 0.35).

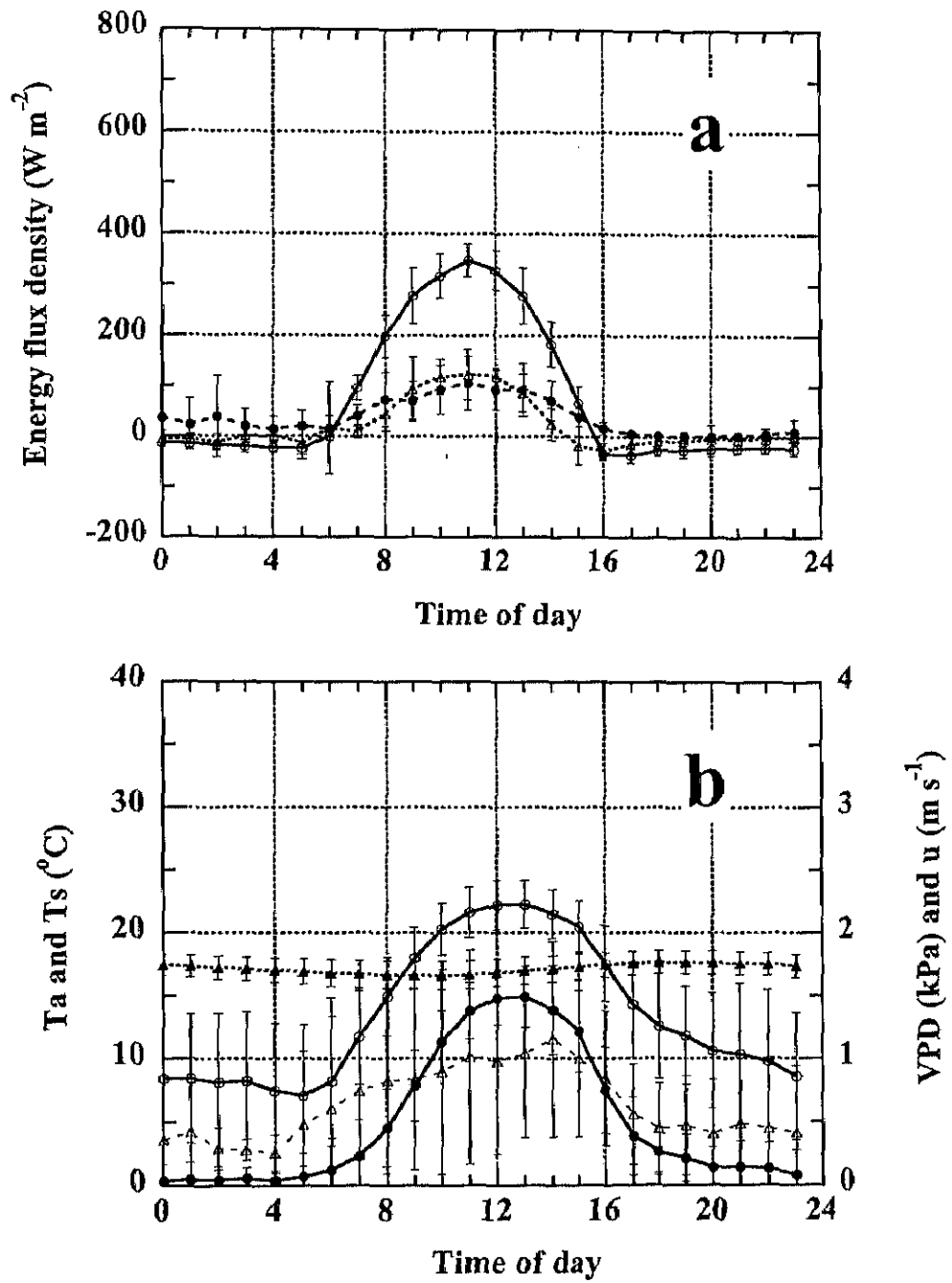


Figure 21. Same as Fig. 17 except for 8 selected days (DOY 291 to 304) in the senescence period ($\text{LAI} = 5.00$, $\text{SWC} = 0.39$).

3.5 Seasonal dynamics of the partitioning of available energy

The energy budgets and the average partitioning of the net available energy (Q_n) into the sensible heat (H) and latent heat (LE) flux densities for the grassland displayed a distinct seasonal pattern, which is reflected in the Bowen ratio (β) and the evaporative fraction (EF) (Table 2).

During the rapid growth period and the closed canopy period, LE dominated the daily energy budget, and midday β s were generally less than 0.60 and approached the minimum in late July to early August (DOY 204 to 216) when the canopy closed and soil moisture was plentiful due to previous *Baiu* rains. During the flowering period and the senescence period, H dominated the daily energy budget; relatively higher values of midday β s were generally observed to be greater than unity on most clear days. EF was generally greater than 50% on most measurement days of the growing period. EF reached its peak values (more than 85%) just after the canopy closed (DOY 204 to 235). The highest value of EF for the ERC grassland was around 90%. EF decreased as the grasses aged. Low EF was observed late in the senescence period (DOY 310 to 320).

Seasonal variations in EF observed in the present study are similar to those reported in the literature for grassland and crops when there is no water limitation. For example, EF ranges between 60% and 80% for a C4-dominated grassland (Verma et al., 1992a); EF varies from 70% to 90% for crops (e.g. Baldocchi, 1994a).

The daily maximal value of LE was *ca.* 540 W m^{-2} on DOY 213 (equivalent to an hourly evapotranspiration rate, ET 0.79 mm h^{-1}). The maximal value of daily accumulative latent heat flux density was $16.28 \text{ MJ m}^{-2} \text{ d}^{-1}$ (6.7 mm d^{-1}) on DOY 231. These values are compatible to the maximal ET rates for grassland in Kelliher et al. (1993), and are rather larger than those observed at a semi-arid grassland in China (Li et al., 2000). The daily maximal ET of this grassland was about 12% larger than that (6.0 mm d^{-1} , Iida, 2000) of the Japanese red pine forest adjacent to the grassland.

Table 2 Daily (24-h) mean integrated values of the energy budget components, partitioning (%) of the net available energy (Q_n , defined as the net radiation flux density minus the soil heat flux density) into the sensible heat (H) and latent heat (LE) flux densities, evaporative fraction (EF , defined as the ratio of LE to Q_n), and Bowen ratios (β) in various growth periods of the ERC grassland in 1999. Also are displayed in this table mean leaf area indices (LAI), daily mean volumetric soil water content (SWC), and solar radiation (R_s). Values in parentheses are standard deviations.

Periods	DOY	LAI	SWC	R_s	Q_n	H	LE	EF	β
					$\text{MJ m}^{-2} \text{d}^{-1}$			%	
Period prior to canopy closure	151-159 (8d)	2.13	0.38	21.9 (± 5.7)	10.5 (± 3.9)	3.3 (± 1.7)	6.9 (± 2.1)	66	0.60
Closed canopy period	204-216 (13d)	5.25	0.37	23.6 (± 3.9)	13.9 (± 3.1)	1.6 (± 2.7)	13.4 (± 3.1)	97	0.32
Closed canopy period	227-235 (9d)	5.50	0.42	20.1 (± 4.5)	11.6 (± 3.2)	2.3 (± 3.1)	11.0 (± 2.9)	95	0.38
Closed canopy period	241-255 (15d)	5.50	0.33	15.2 (± 4.7)	9.0 (± 3.3)	2.9 (± 3.2)	7.0 (± 2.8)	77	0.59
Flowering period	271-290 (11d)	5.37	0.35	15.0 (± 3.2)	8.0 (± 2.3)	4.1 (± 4.2)	4.5 (± 2.3)	57	1.17
Senescence period	291-304 (8d)		0.39	14.5 (± 1.9)	6.4 (± 1.9)	1.8 (± 2.3)	3.2 (± 2.8)	51	1.20

3.6 Diurnal patterns of net canopy CO₂ flux density over the grassland

Diurnal patterns of net canopy CO₂ flux density (F_c) measured over the grassland were very similar to each other in shape but varied substantially in amplitude depending on growth status of the canopy during the measurements (Figs. 22 to 26). Because no water stress occurred in the ERC grassland, both F_c and PPFD followed similar patterns in diurnal variations, exhibiting their close coupling (Figs. 22 to 26).

During most time of the day, the canopy assimilated more CO₂ via photosynthesis than that released via respiration from plants and the soil. The canopy released CO₂ only to the ambient through the respiration at night. During the morning hours, F_c switched sign (from a source to a sink of CO₂) 1 to 2 h after sunrise, increased rapidly thereafter with the rapid increase of PPFD, and then approached its peak values at solar noon (about 11:00 Japanese Standard Time, JST hereinafter) as PPFD did. During the afternoon hours, F_c decreased precipitously in response with rapid diminution of PPFD and switched sign again (from a sink to a source of CO₂) 1 to 3 h before sunset. F_c reached zero when PPFD was still substantially large as a consequence of higher respiration rate from grasses and the soil than the canopy photosynthetic rate. The magnitudes of F_c when PPFD approached $0 \mu \text{mol m}^{-2} \text{s}^{-1}$ in the late afternoon was larger than those in the early morning. Meanwhile, the magnitudes of PPFD when F_c approached $0 \mu \text{mol m}^{-2} \text{s}^{-1}$ (“canopy light compensation point, LCP”) was larger in the late afternoon than in the early morning (Table 4), because the relatively higher temperature in the late afternoon was more favorable to respiration as compared to the early morning when the air temperatures were lowest in the day. These properties resulted in a slight asymmetrical distribution of F_c in the daytime.

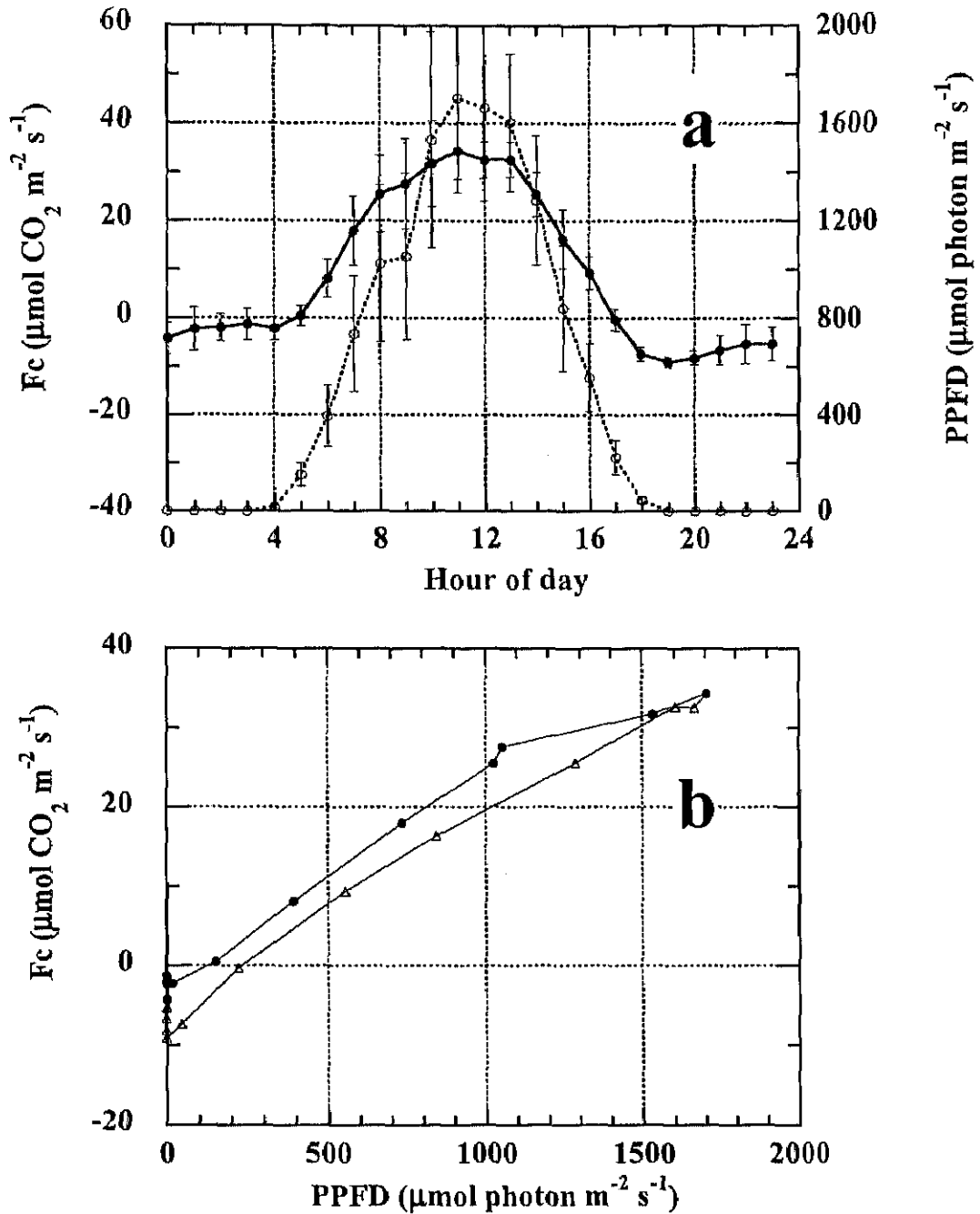


Figure 22. a: Daily courses of the net canopy CO₂ flux (F_c , solid line with ●) and photosynthetic photon flux density (PPFD, dashed line with ○) for selected clear days in the rapid growth period (DOY 151 to 159, 9 days, LAI = 2.13, Mean volumetric soil water content, SWC was 0.38). Positive values signify carbon gain of the canopy from the atmosphere and negative values indicate carbon release from the canopy to the atmosphere. Vertical bars in the figure indicate standard deviations of hourly mean. b: the relationship between F_c and PPFD over the same period and morning and afternoon data are denoted with solid circle (●) and triangle (△), respectively.

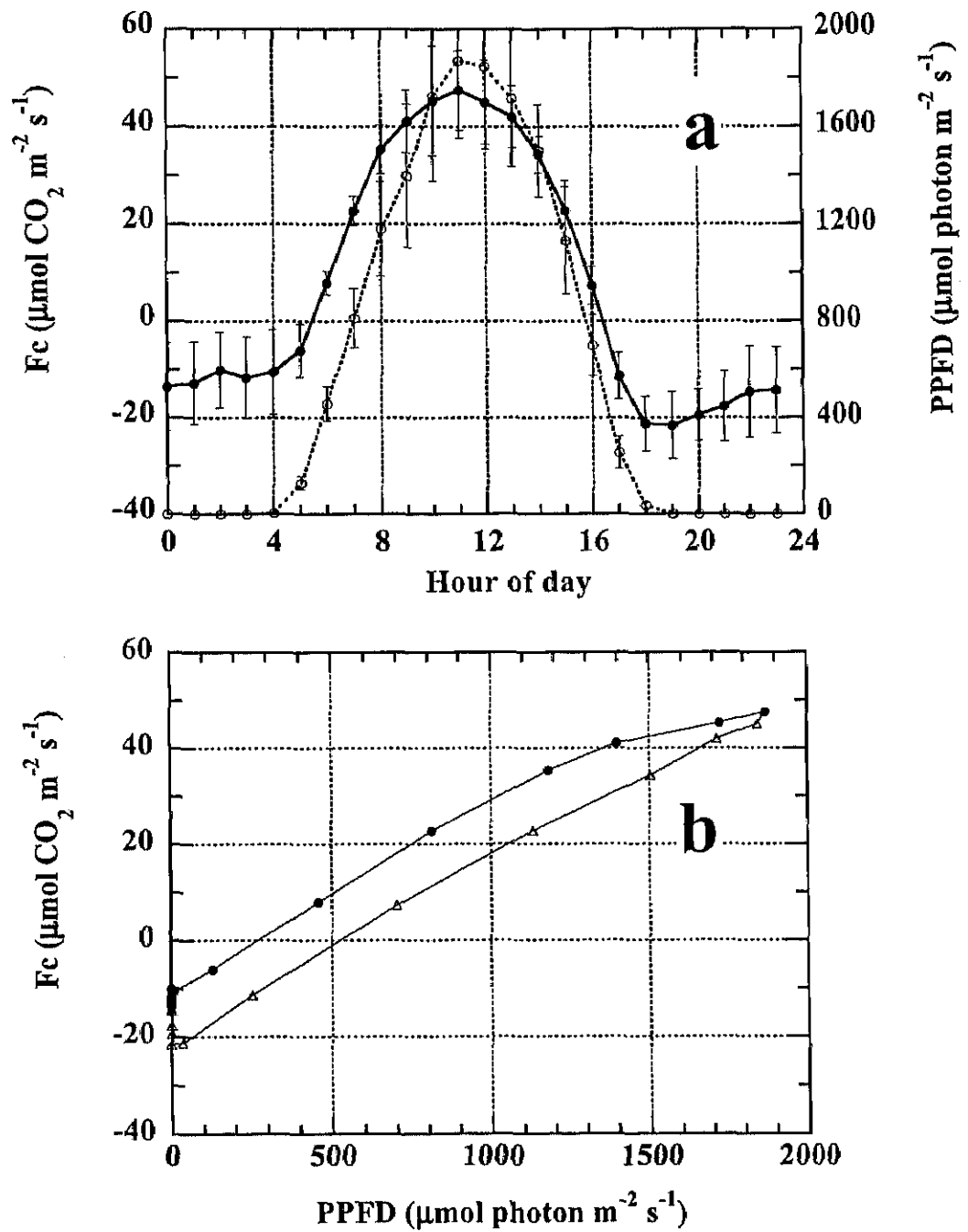


Figure 23. Same as Fig 22 but for the early part of the closed canopy period (DOY 204 to 216, 13 days, LAI = 5.25, SWC = 0.37).

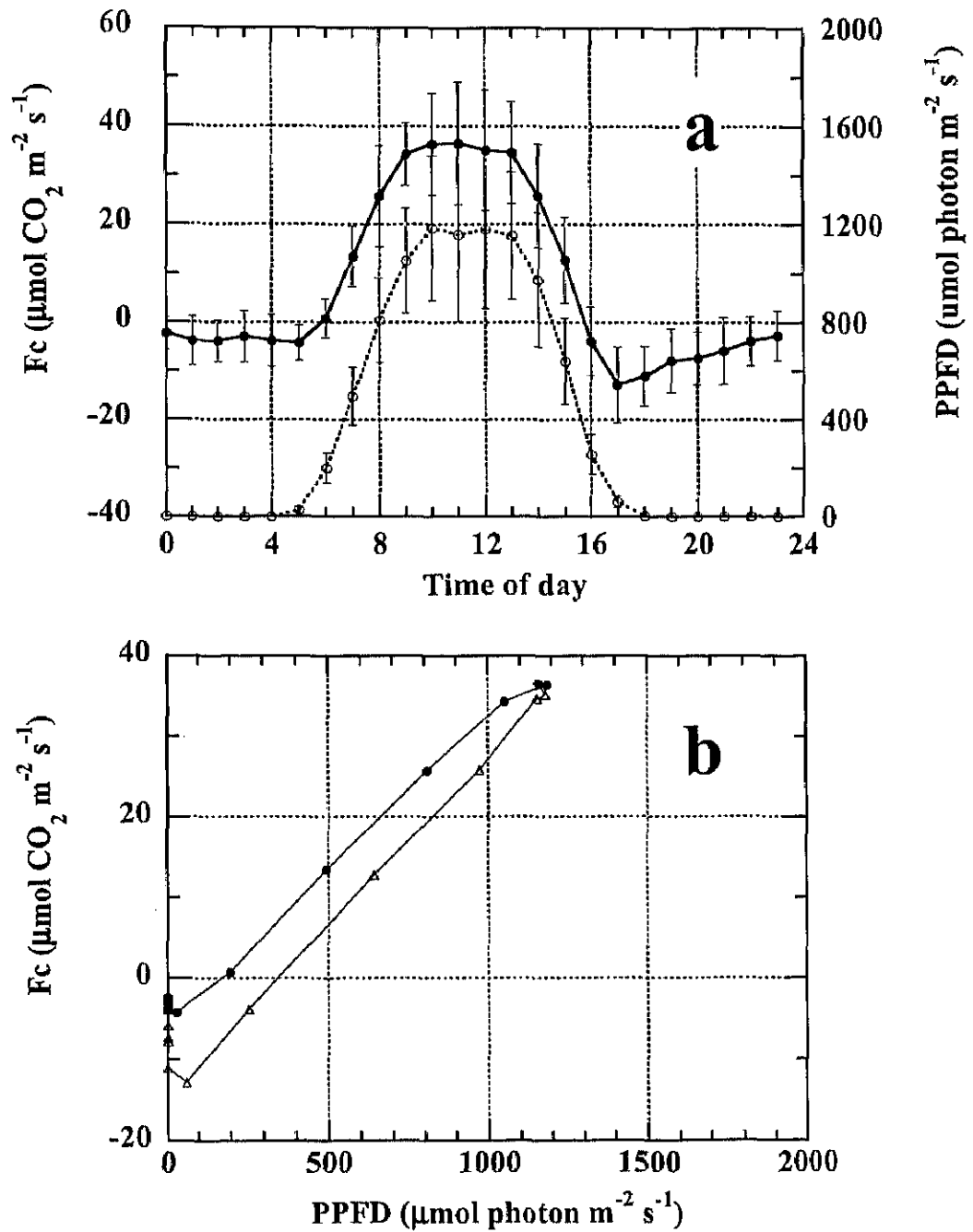


Figure 24. Same as Fig 22 but for the later part of the closed canopy period (DOY 241 to 255, 15 days, LAI = 5.50, SWC = 0.33).

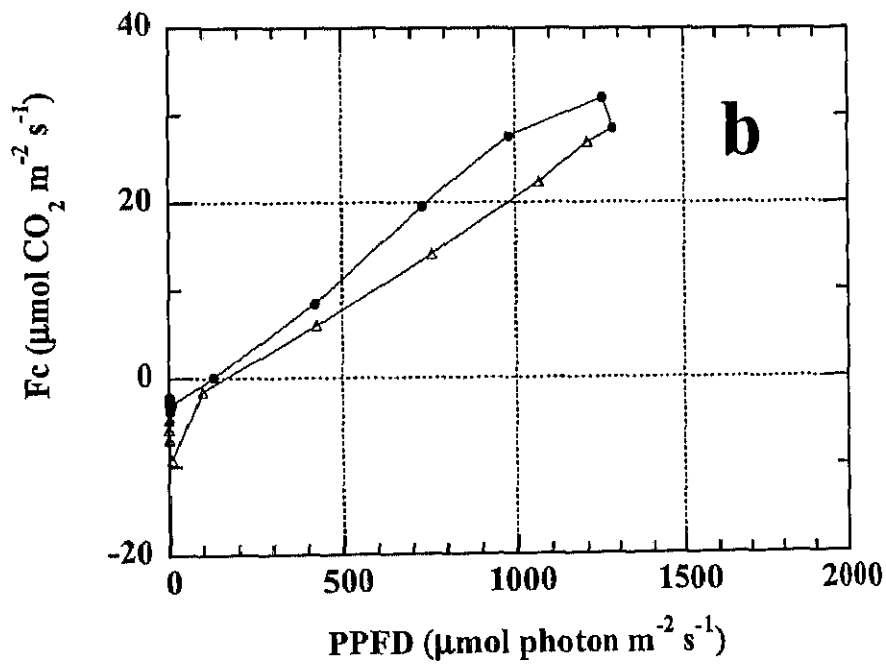
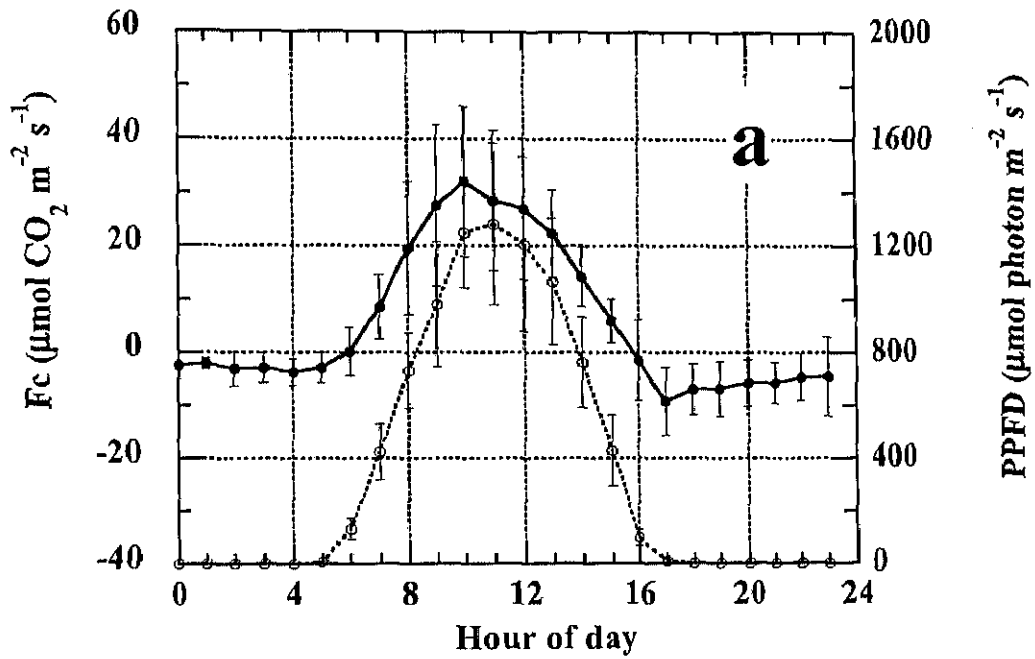


Figure 25. Same as Fig 22 but for the flowering period (DOY 271 to 290, 8 days, LAI = 5.37, SWC = 0.35).

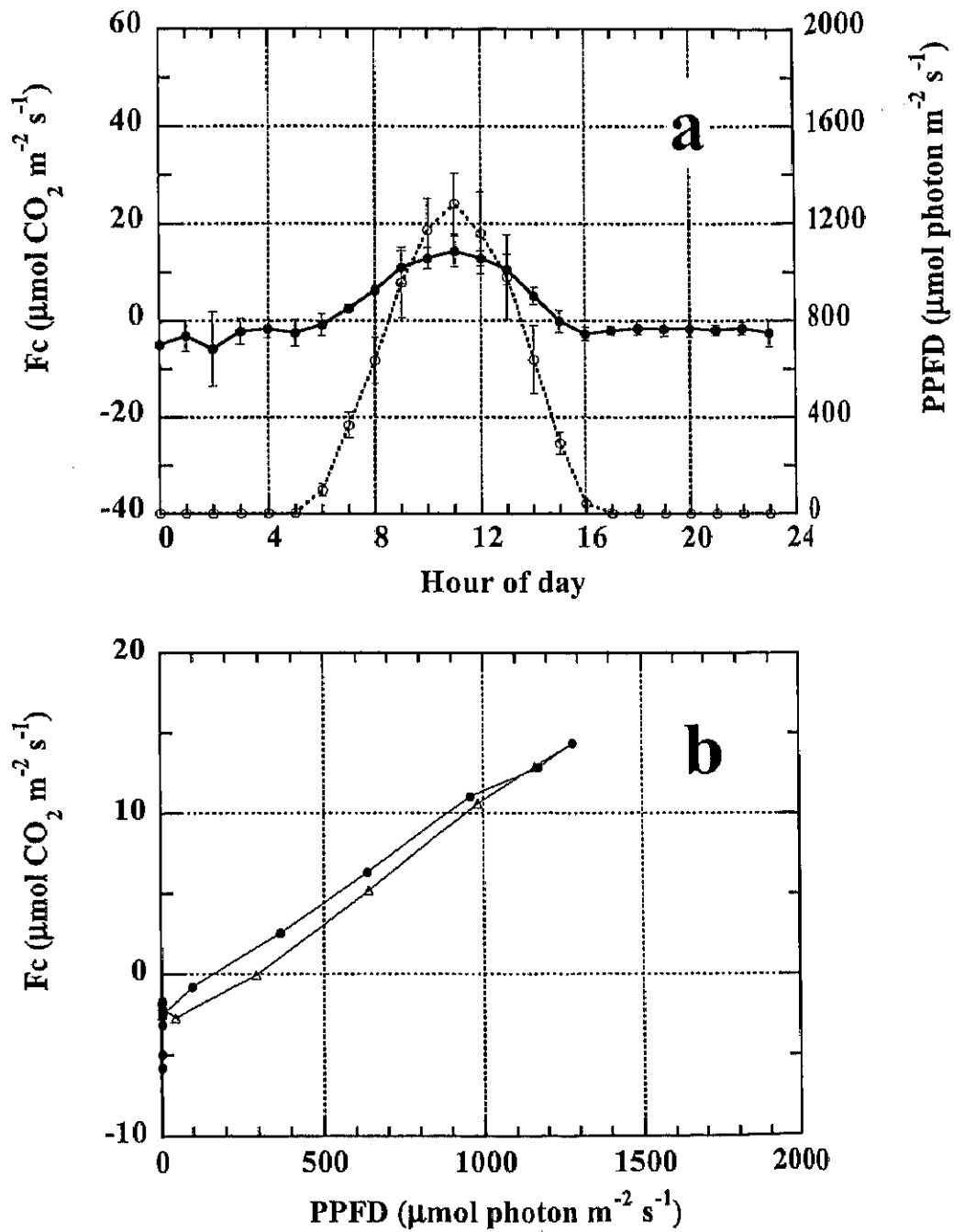


Figure 26. Same as Fig 22 but for the senescence period (DOY 291 to 304, 8 days, LAI = 5.00, SWC = 0.39).

Absolute values of dark respiration generally reached the largest just after sunset, decreased gradually until midnight and then remained relatively stable throughout the rest of night. The grassland was usually a sink for atmospheric CO₂ in daytime.

Daily courses and magnitudes of F_c , and sink duration (net carbon gain time) differed depending on the growth stages of grasses (Table 3). Maximal daytime F_c values varied between 7.3 (DOY 304) and 56.7 $\mu\text{ mol m}^{-2} \text{ s}^{-1}$ (DOY 231), and nighttime F_c values varied from -1.3 to -21.6 $\mu\text{ mol m}^{-2} \text{ s}^{-1}$ (Table 3).

During the rapid growing period (DOY 151 to 159), peak values of F_c ranged from 30 to 42 $\mu\text{ mol m}^{-2} \text{ s}^{-1}$ (1.3 to 1.8 $\text{mg m}^{-2} \text{ s}^{-1}$). Maximal PPFD value was around 2210 $\mu\text{ mol m}^{-2} \text{ s}^{-1}$. Daily maximum integrated value of F_c over the grassland during this period was 0.96 $\text{mol m}^{-2} \text{ d}^{-1}$ (DOY 150, 42.3 $\text{g m}^{-2} \text{ d}^{-1}$). Minimum integrated value of daily F_c -0.20 $\text{mol m}^{-2} \text{ d}^{-1}$ (-9.0 $\text{g m}^{-2} \text{ d}^{-1}$) over the grassland was observed on DOY 158 when it was cloudy with a thunder (8.1 mm). On clear days, the canopy shifted from a source to a sink about 05:00 JST, and from a sink to a source about 16:00 JST. Sink duration on clear days was about 12 h in this period. Values of F_c at PPFD = 0 were about -1.31 $\mu\text{ mol m}^{-2} \text{ s}^{-1}$ in the morning and about -9.13 $\mu\text{ mol m}^{-2} \text{ s}^{-1}$ in the afternoon, respectively. Nighttime CO₂ flux density due to respiration from soil and grasses during this period ranged from -1.31 to -9.13 $\mu\text{ mol m}^{-2} \text{ s}^{-1}$.

During the early part of the closed canopy period (DOY 204 to 243), peak values of F_c ranged from 40 to 58 $\mu\text{ mol m}^{-2} \text{ s}^{-1}$ (1.8 to 2.6 $\text{mg m}^{-2} \text{ s}^{-1}$). Maximal PPFD value was about 2190 $\mu\text{ mol m}^{-2} \text{ s}^{-1}$. Daily maximum integrated value of F_c over the grassland during this period was 1.06 $\text{mol m}^{-2} \text{ d}^{-1}$ (DOY 234, 46.6 $\text{g m}^{-2} \text{ d}^{-1}$). On clear days, F_c was positive from about 05:00 to 17:00 h JST. Sink duration on clear days was about 13 h in this period. Values of F_c at PPFD = 0 were about -11.70 $\mu\text{ mol m}^{-2} \text{ s}^{-1}$ in the morning and about -21.60 $\mu\text{ mol m}^{-2} \text{ s}^{-1}$ in the afternoon, respectively. Nighttime CO₂ flux density during this period was from -6.06 to -21.60 $\mu\text{ mol m}^{-2} \text{ s}^{-1}$. The amplitude of F_c was largest in this growth period ranging from -22 to 60 $\mu\text{ mol m}^{-2} \text{ s}^{-1}$. Even though the amount of incipient PPFD was higher during this period, the net CO₂ flux

density was lower than that during the rapid growing period, implying that the respiration from soil and plants could account for loss of carbon. It is also reflected in the carbon gain and loss analysis in Table 4.

During the late part of the closed canopy period (DOY 244 to 270), peak values of F_c ranged from 30 to 60 $\mu\text{ mol m}^{-2} \text{ s}^{-1}$ (1.4 to 2.6 $\text{mg m}^{-2} \text{ s}^{-1}$). Maximal *PPFD* value was about 1720 $\mu\text{ mol m}^{-2} \text{ s}^{-1}$. Daily maximum integrated value of F_c over the grassland during this period was 1.00 $\text{mol m}^{-2} \text{ d}^{-1}$ (DOY 248, 44.0 $\text{g m}^{-2} \text{ d}^{-1}$). Sink duration on clear days was about 11 h (from 06:00 to 16:00 h JST) in this period. Values of F_c at *PPFD* = 0 were about $-3.80 \mu\text{ mol m}^{-2} \text{ s}^{-1}$ in the morning and about $-11.10 \mu\text{ mol m}^{-2} \text{ s}^{-1}$ in the afternoon, respectively. Dark CO_2 flux density varied between -2.93 and $-12.89 \mu\text{ mol m}^{-2} \text{ s}^{-1}$. This period was also characterized by large daytime carbon gains by the canopy accompanied with large nighttime carbon losses from the soil and the canopy due to respiration.

During the flowering period (DOY 271 to 290), peak values of F_c ranged from 15 to 59 $\mu\text{ mol m}^{-2} \text{ s}^{-1}$ (0.7 to 2.6 $\text{mg m}^{-2} \text{ s}^{-1}$). Maximal *PPFD* value was 1610 $\mu\text{ mol m}^{-2} \text{ s}^{-1}$. Daily maximum integrated value of F_c over the grassland during this period was 0.94 $\text{mol m}^{-2} \text{ d}^{-1}$ (DOY 273, 41.5 $\text{g m}^{-2} \text{ d}^{-1}$). Daily minimum integrated value of F_c $-0.46 \text{ mol m}^{-2} \text{ d}^{-1}$ ($-20.1 \text{ g m}^{-2} \text{ d}^{-1}$) over the grassland was observed on DOY 276 when it was cloudy. On clear days, Positive time length for F_c was about 10 h (from 06:00 to 15:00 h JST). Values of F_c at *PPFD* = 0 were about $-3.73 \mu\text{ mol m}^{-2} \text{ s}^{-1}$ in the morning and about $-6.99 \mu\text{ mol m}^{-2} \text{ s}^{-1}$ in the afternoon, respectively. Nighttime CO_2 flux density ranged from -2.12 to $-9.23 \mu\text{ mol m}^{-2} \text{ s}^{-1}$.

During the senescence period (DOY 291 to 346), peak values of F_c ranged from 8 to 18 $\mu\text{ mol m}^{-2} \text{ s}^{-1}$ (0.4 to 0.8 $\text{mg m}^{-2} \text{ s}^{-1}$). Maximal *PPFD* value was 1420 $\mu\text{ mol m}^{-2} \text{ s}^{-1}$. Daily maximum integrated value of F_c over the grassland during this period was 0.20 $\text{mol m}^{-2} \text{ d}^{-1}$ (DOY 315, 8.6 $\text{g m}^{-2} \text{ d}^{-1}$). On clear days, the transition time from source to sink in the morning was generally about 07:00 JST, and the transition time from sink to source in the afternoon was generally about 14:00 JST. Sink duration on

clear days was about 8 h (07:00 to 14:00 h JST) in this period. A general large decrease in F_c during the senescent period can be reasonably due to low levels of PPFD, low air temperatures (frost events), and the reduction in photosynthetic capacity of grasses as a result of aging. Values of F_c at PPFD = 0 were about $-1.16 \mu \text{ mol m}^{-2} \text{ s}^{-1}$ in the morning and about $-2.06 \mu \text{ mol m}^{-2} \text{ s}^{-1}$ in the afternoon, respectively. Nighttime CO_2 flux density varied from -1.16 to $-5.80 \mu \text{ mol m}^{-2} \text{ s}^{-1}$.

Table 3 Diurnal characteristics of the net canopy CO₂ flux (F_c) on clear days. PPF_{Dmax}, maximum PPF; T_{len} , mean time length for net carbon gain ($F_c > 0$); F_{cmax} , peak values of daytime F_c ; R_N , amplitude of nighttime F_c ; and NEE_{max}, maximum values of the daily integrated F_c . Values in parenthesis indicate DOY.

Period	DOY	PPFD _{max}	T_{len}	F_{cmax}	R_N	NEE _{max}
		$\mu \text{ mol m}^{-2} \text{ s}^{-1}$	<i>h</i>	$\mu \text{ mol m}^{-2} \text{ s}^{-1}$	$\mu \text{ mol m}^{-2} \text{ s}^{-1}$	$\text{mol m}^{-2} \text{ d}^{-1}$
Prior to canopy closure	151–159	2200 (159)	12	30.07 (154)~41.32 (157)	-1.31 ~ -9.13	0.96 (152)
Early closed canopy	204–243	2190 (213)	13	41.49 (215)~57.43 (242)	-6.06 ~ -21.60	1.06 (234)
Late closed canopy	244–270	1960 (244)	11	29.70 (244)~59.22 (257)	-2.93 ~ -12.89	1.00 (248)
Flowering	271–290	1610 (273)	10	14.31 (271)~58.38 (287)	-2.12 ~ -9.23	0.94 (273)
Senescence	291–304	1410 (294)	8	7.28 (304)~17.24 (297)	-1.66 ~ -5.80	0.21 (302)

3.7 Seasonal dynamics of the net canopy CO₂ flux density

Mean daily-integrated net canopy CO₂ flux density (NEE) over the ERC grassland showed a distinct seasonal pattern (Table 4). NEE was largest ($0.75 \pm 0.36 \text{ mol m}^{-2} \text{ d}^{-1}$) in the rapid growth period. This may be attributed to optimal microenvironmental and eco-physiological conditions during this period, for example, higher PPFD, ample soil moisture, vigorous photosynthetic activity, and relatively lower respiration due to grasses and the soil. Net carbon losses accounted for about 21% of net carbon gains during this period.

The early closed canopy period had a characteristic of larger daytime carbon gains to the canopy in conjunction with larger nighttime carbon losses from the canopy so that the NEE ($0.60 \pm 0.58 \text{ mol m}^{-2} \text{ d}^{-1}$) was lower than that in the rapid growing period. Net carbon losses due to respiration were equivalent to 52% of net carbon gains. Higher carbon gains were probably explained by the fact that the canopy was well developed with vigorous photosynthetic activity, PPFD was considerably higher, and soil moisture was plentiful just after the end of the *Baiu* rain period. Higher carbon losses were mainly due to higher temperatures that were closely correlated with respiration. Plentiful soil moisture might also enhance soil microbiotic activities that enhanced emission of CO₂ from the soil due to respiration. Obviously, the factors that increased the canopy photosynthesis (e.g. higher incident PPFD, wet soil, and higher temperature) also enhanced CO₂ release from the canopy by means of respiration. If we assume that the same amount of nighttime F_c is maintained during the daytime, then the rate of net photosynthesis (A_c) of the canopy is very high at this growth stage of grasses, at least greater than the sum of absolute daytime F_c and absolute nighttime F_c . Leaf litter decomposition during this period might be rapid due to higher temperatures and ample soil moisture, which might contribute to some extent to higher carbon losses from the canopy.

With progression of the growing season, the canopy photosynthetic capacity decreased, so that the net canopy CO₂ flux density decreased. For example, NEE decreased to $0.44 \pm 0.56 \text{ mol m}^{-2} \text{ d}^{-1}$ on clear days during the flowering period. The absolute values of the respiration decreased too during this period; net carbon losses were about one third of net carbon gains. NEE was lowest ($< 0.15 \text{ mol m}^{-2} \text{ d}^{-1}$) as the canopy senesced, and about 48% of net carbon gains were offset by net carbon losses. Lower F_c during the later growing period may also be attributable to lower PPF and lower temperatures. The canopy often experienced air temperatures lower than 5 °C from 18 October 1999 when *Solidago altissima* (a dominant C3 species) started dropping leaves and leaves of *Imperata cylindrical* (C4) and *Miscanthus sinensis* (C4) were yellowing. Several frosts occurred from mid-November. Most plants were dead by the end of November except *Festuca arundinacea* (C3), which survived throughout the year. During this period, nearly all the carbon gained by the remaining living grasses was lost due to respiration.

Additionally, cloudiness in the sky affected the patterns of canopy CO₂ sink and source. F_c was appreciably decreased on cloudy days. The canopy often became a source of CO₂ on overcast days when air temperature and corresponding VPD decreased (Table 4). For example, NEE values were $-0.20 \text{ mol m}^{-2} \text{ d}^{-1}$ on cloudy DOY 150 and $-0.46 \text{ mol m}^{-2} \text{ d}^{-1}$ on cloudy DOY 276. However, the canopy was a sink for CO₂ during most of the growing period.

The results obtained in the present study were compared to those reported in recent literature for other types of canopy. Maximal values of the canopy CO₂ flux density for the ERC grassland varied from 10 to $63 \mu \text{ mol m}^{-2} \text{ s}^{-1}$ (0.7 to $2.6 \text{ mg m}^{-2} \text{ s}^{-1}$) during the 1999 growing season. Daily-integrated values (NEE) of F_c ranged from 0.14 to $0.64 \text{ mol m}^{-2} \text{ d}^{-1}$ (6.2 to $28.2 \text{ g m}^{-2} \text{ d}^{-1}$) with a maximum of $1.06 \text{ mol m}^{-2} \text{ d}^{-1}$ ($46.8 \text{ g m}^{-2} \text{ d}^{-1}$, DOY 234). Values of F_c and NEE in the present study were slightly greater than those observed in 1993 and 1994 at the same grassland by Saigusa et al. (1998) using the profile method. This is probably due to differences in LAI during the measurements.

Maximal LAI was 5.5 in 1999, but it is 3.4 and 4.5 in 1993 and in 1994, respectively (Saigusa et al., 1998). The data presented here are compatible in magnitude to those reported in the literature for grasslands and crops grown under no water limiting conditions (Baldocchi, 1994b). For example, maximal values of net CO₂ flux density were 45 to 68 $\mu\text{ mol m}^{-2} \text{ s}^{-1}$ for a wheat (C3) canopy with LAI varying 2.7 to 3.3 and without water stress, and maximal integration of diurnal CO₂ flux density (NEE) yields around 1.12 mol CO₂ m⁻² d⁻¹ (Baldocchi, 1994b; Baldocchi et al., 1981b; Kim and Verma, 1990b).

Table 4 Mean values of the daily-integrated (24-h) net canopy CO₂ flux (NEE), net canopy carbon gain ($F_c > 0$, sink) and loss ($F_c < 0$, source) and their ratio (-/+), and water use efficiency (WUE). Mean values of leaf area index (LAI), daily means of 1.6-m air temperature (T_a) and 2-cm soil temperature (T_s), daily mean volumetric soil water content (SWC), daily-integrated photosynthetic photon flux density (PPFD), and light compensation point in the morning (LCP_{am}) and in the afternoon (LCP_{pm}), are also displayed. Values in parentheses are standard deviations.

Period	DOY	LAI	SWC	T_a	T_s	PPFD	$F_c > 0$	$F_c < 0$	NEE	-/+	LCP _{am}	LCP _{pm}	WUE
				°C			mol m ⁻² d ⁻¹				μ mol m ⁻² s ⁻¹		mg g ⁻¹
Prior canopy closure	to 51–159 (8d)	2.13	0.38	21.3	22.1	46.21	0.95	-0.20	0.75	0.21	128.3	242.5	16.5
				(±2.2)(±0.9)(±12.00)					(±0.36)				(±2.9)
Closed canopy	104–216 (13d)	5.25	0.37	28.3	27.4	53.17	1.26	-0.66	0.60	0.52	272.2	527.8	12.0
				(±0.9)(±0.2)(±9.40)					(±0.58)				(±1.6)
Closed canopy	227–235 (9d)	5.50	0.42	27.9	27.9	45.17	1.08	-0.44	0.64	0.41	178.0	515.6	12.5
				(±1.1)(±0.2)(±10.44)					(±0.59)				(±3.0)
Closed canopy (Cloudy days)	236–240 (5d)	5.50	0.36	25.4	27.2	25.71	0.62	-0.40	0.22	0.65	180.4	253.9	17.9
				(±1.3)(±0.4)(±12.67)					(±0.53)				(±4.7)
Closed canopy	241–255 (15d)	5.50	0.33	25.6	26.1	33.09	0.92	-0.28	0.64	0.30	174.3	352.7	17.0
				(±2.1)(±0.8)(±10.35)					(±0.61)				(±4.1)
Flowering	271–290 (11d)	5.37	0.35	19.7	22.4	30.18	0.66	-0.22	0.44	0.33	126.7	165.0	18.7
				(±3.4)(±1.6)(±7.03)					(±0.56)				(±9.1)
Flowering (Cloudy days)	271–290 (8d)	5.37	0.35	17.9	22.2	10.53	0.21	-0.27	-0.06	1.29	93.7	271.1	14.2
				(±3.3)(±1.3)(±6.28)					(±0.58)				(±10.0)
Senescence	291–304 (8d)		0.39	13.5	17.2	27.57	0.27	-0.13	0.14	0.48	162.2	297.8	16.2
				(±3.9)(±1.0)(±4.02)					(±0.20)				(±6.6)

3.8. Water use efficiency (WUE)

One approach to link CO₂ flux density with H₂O flux density is through the index of water use efficiency (WUE). The highest WUE values were generally observed in the mid-morning hours (usually between 06:00 and 10:00 JST) and declined in the afternoon (Fig. 27). Diurnal trends of WUE and canopy surface conductance (g_c) followed a similar pattern (data not shown here graphically). Higher values of WUE in the mid-morning were presumably due to lower VPD and more widely open of stomata while lower WUE values in the late afternoon were probably caused by higher VPD (accompanied by higher air temperatures) and partial stomatal closure, which restricted carbon fixation but induced much water loss from the soil (Baldocchi et al., 1985; Jones, 1992; Moncrieff et al., 1997). Stronger winds in the afternoon favored evaporation. Frequent occurrence of sensible heat advection (SHA) at the ERC grassland was reasonably one of major determinants to account for sharp decline of WUE in the afternoon hours since the energy produced by SHA enhanced water loss from the canopy (Anderson et al., 1984; Baldocchi et al., 1981a, b).

On a seasonal time scale, WUE generally varied from 12 to 19 mg CO₂ (g H₂O)⁻¹ (Table 4). Lower WUE values observed in the early closure period may have been due largely to much water loss from soil evaporation accompanied with higher temperature and corresponding higher VPD just after the end of the *Baiu* rain period. Note that relatively higher WUE values were also observed during the flowering period and the senescent period, this may be possibly ascribed to decrease of VPD accompanied by lower temperatures that resulted in decrease of ET. WUE observed at the ERC grassland was slightly greater than those for crops (5 to 15 mg CO₂ g⁻¹ H₂O) (e.g. Anderson et al., 1984; Baldocchi, 1994b).

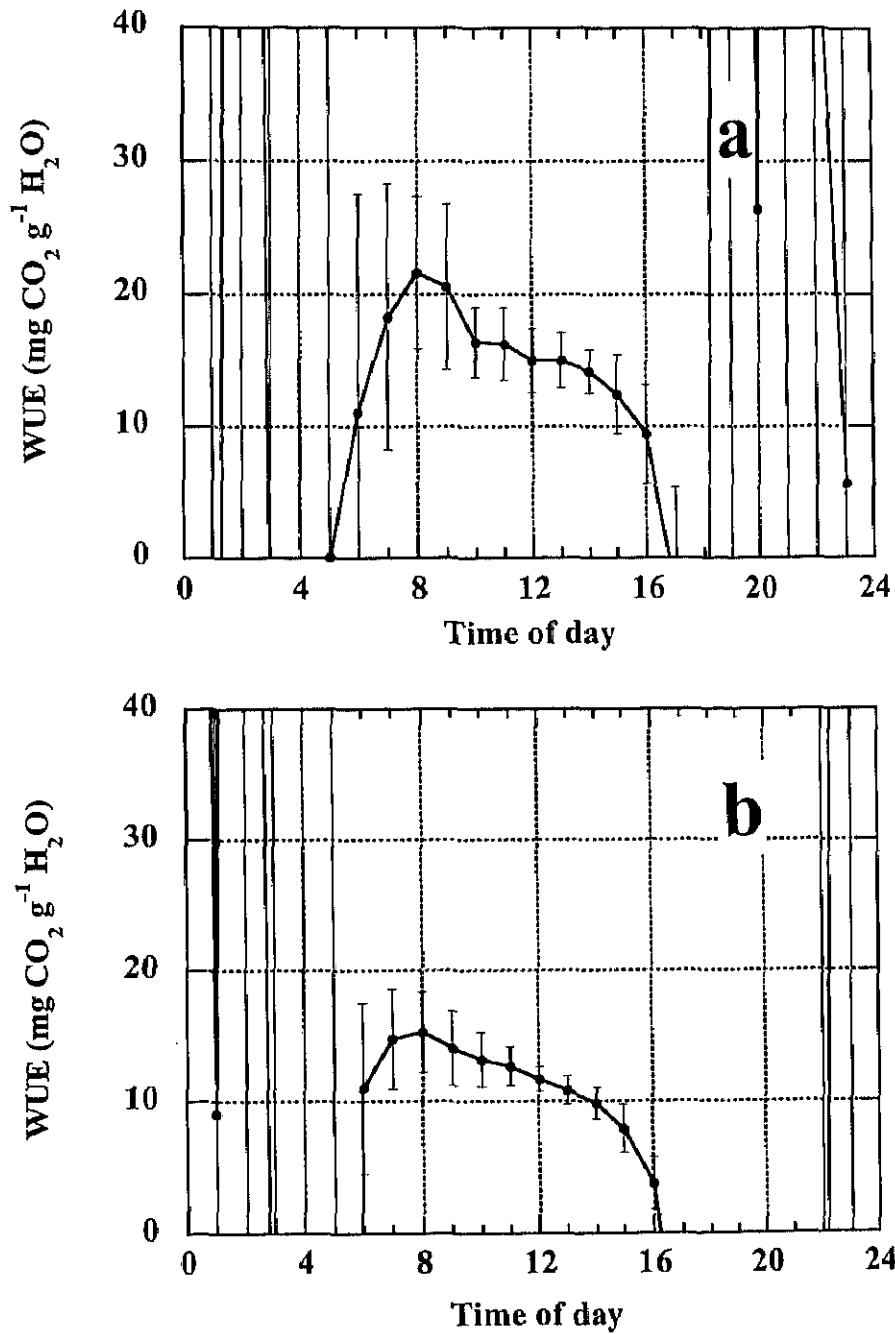


Figure 27. Diurnal variations in water use efficiency (WUE) for selected clear days. a: the period prior to canopy closure (DOY 151 to 159, 9 days, LAI = 2.13). b: the closed canopy period (DOY 204 to 216, 13 days, LAI = 5.25).